



DIPLOMARBEIT

Various bijections between maps and tree-like structures

zur Erlangung des akademischen Grades

Master of Science

im Rahmen des Studiums

Technische Mathematik

ausgeführt am

Institut für Diskrete Mathematik und Geometrie TU Wien

unter der Anleitung von

Univ.Prof. Dipl.-Ing. Dr.techn. Michael Drmota

durch

Christian Göth, BSc

Matrikelnummer: 11811883

Kurzfassung

Diese Arbeit befasst sich mit Bijektionen zwischen planaren maps und baumartigen Strukturen, ein essentielles Konzept der modernen Kombinatorik mit Verbindungen zur Wahrscheinlichkeitstheorie und zur statistischen Physik. Seit Tuttes bahnbrechenden Arbeiten zur Enumeration planarer Maps wurden von verschiedenen Autoren zahlreiche bijektive Methoden entwickelt. In dieser Arbeit werden diese Ansätze gesammelt und präsentiert, mit dem Ziel, ihre gemeinsamen Prinzipien und charakteristischen Unterschiede hervorzuheben. Zu diesem Zweck führen wir einheitliche Notationen ein und unterscheiden zwei Hauptkategorien von Bijektionen: (A) Blossoming-Tree-Bijektionen, bei denen Karten durch dekorierte Spannbäume codiert werden, und (B) Nicht-Spannbaum-Bijektionen, bei denen alternative Strukturen wie well-labeled Bäume oder Mobiles verwendet werden. Für jede Kategorie beschreiben wir ein vereinheitlichtes Schema, das die Essenz der bijektiven Konstruktionen erfasst und aufzeigt, wie verschiedene Resultate in dieses Gesamtbild passen.

Anwendungen dieser Bijektionen zur Enumeration werden anschließend im Detail diskutiert. Zunächst betrachten wir klassische Resultate wie die Enumeration gewurzelter Eulerscher Maps und Quadrangulierungen, die bereits mit anderen Methoden hergeleitet wurden. Die Bijektionen liefern dabei nicht nur bekannte Abzählformeln, sondern ermöglichen auch ein tieferes konzeptionelles Verständnis der speziellen Struktur dieser Formeln. Abschließend gehen wir kurz auf geometrische Aspekte ein, insbesondere darauf, wie Bijektionen wie die Korrespondenz von Cori-Vauquelin-Schaeffer als Ausgangspunkt für die Analyse von Abständen in zufälligen planaren Maps und für Resultate zu Skalierungs-Limits dienen, die zur sogenannten Brown'schen Map konvergieren. Anstelle vollständiger Beweise dieser probabilistischen Resultate liegt der Fokus der Arbeit auf dem kombinatorischen Hintergrund, der notwendig ist, um zu verstehen, wie bijektive Methoden das Studium der Zufallsgeometrie unterstützen.

Abstract

This thesis investigates bijections between planar maps and tree-like structures, an essential concept in modern combinatorics with connections to probability theory and statistical physics. Since Tutte's pioneering work on the enumeration of planar maps, many bijective approaches have been developed by different authors, and here we collect and present a variety of them, with the aim of highlighting their common principles and distinctive features. To this end, we introduce a unified notation and distinguish two main categories of bijections: (A) blossoming-tree bijections, where maps are encoded by decorated spanning trees, and (B) non-spanning-tree bijections, where encodings rely on alternative structures such as well-labeled trees or mobiles. For each category, we describe a unified scheme that captures the essence of the bijective constructions and illustrates how different results fit into this broader picture.

Applications of these bijections to enumeration purposes are then discussed in detail. First, we revisit classical results as the enumeration of rooted Eulerian maps and quadrangulations that have already been derived using other approaches. The bijections not only recover known counting formulas, but also provide a deeper conceptual understanding of the specific structural form of these formulas. Finally, we briefly touch upon geometric aspects, in particular, how bijections such as the Cori-Vauquelin-Schaeffer correspondence serve as a starting point for the analysis of distances in random planar maps and for scaling-limit results leading to the Brownian map. Rather than giving full proofs of these probabilistic results, the thesis focuses on providing the combinatorial background needed to understand how bijective methods support the study of random geometry.

Acknowledgement

I would like to express my deepest gratitude to my supervisor, Professor Dr. Michael Drmota, for introducing me to the fascinating topic. His guidance and valuable feedback were essential for the development of this thesis.

I also want to thank my colleagues and friends who not only provided encouragement and advice but also made this journey over the past years enjoyable with their companionship and support.

Finally, my heartfelt thanks also go to my family, who have always supported me unconditionally during my studies. I am deeply grateful for always believing in me.

Eidesstattliche Erklärung

Ich erkläre an Eides statt, dass ich die vorliegende Diplomarbeit selbständig und ohne fremde Hilfe verfasst, andere als die angegebenen Quellen und Hilfsmittel nicht benutzt bzw. die wörtlich oder sinngemäß entnommenen Stellen als solche kenntlich gemacht habe.

Signatur.png

Wien, im August 2025

Contents

1 Introduction			n	1
2	Preliminaries 2.1 Planar maps			3 12
3	Overview of bijections between maps and tree-like structures			15
	3.1	Bijecti	ons of category (A)	15
		3.1.1	Schaeffer's construction for Eulerian maps	15
		3.1.2	Triangulations	19
		3.1.3	Unified bijective scheme	23
		3.1.4	p-gonal d -angulations	27
		3.1.5	Generalization to maps of higher genus	31
	3.2	Bijecti	ons of category (B)	35
		3.2.1	The CVS Bijection	36
		3.2.2	The BDG Bijection	39
		3.2.3	Unified bijective scheme	42
		3.2.4	p-gonal d -angulations	46
		3.2.5	Maps of girth d with root face degree d	48
		3.2.6	Generalization to maps of higher genus	49
4	Selected proofs			
	4.1	Proof	of the CVS Bijection	53
	4.2	Proof	of the unified bijective scheme of category (A)	57
5	Applications			59
	5.1	Enume	eration of Maps	59
		5.1.1	Rooted Eulerian planar maps	59
		5.1.2	Rooted simple triangulations	60
	5.2	Intrins	sic geometries of planar quadrangulations and maps	61
		5.2.1	Distances in planar maps	61
		5.2.2	The Brownian map as a universal scaling limit	62
Re	References			

Introduction

The study of planar maps (graphs embedded in the sphere up to orientation-preserving homeomorphisms) has been a central theme in modern combinatorics since the pioneering work of Tutte in the 1960s. Tutte's recursive decomposition methods led to functional equations for generating functions of maps, from which many remarkable enumeration formulas could be extracted [Tut63]. These results motivated decades of research at the intersection of combinatorics, probability theory, and statistical physics, where planar maps play an important role as discrete models of random surfaces.

A major breakthrough was the development of bijective methods, initiated in the works of Cori, Vauquelin [CV81], Schaeffer [Sch97; Sch98] and later Bouttier, Di Francesco, Guitter [BFG04]. These approaches provide very direct correspondences between planar maps and simpler tree-like structures, replacing analytic arguments by explicit combinatorial encodings. Such bijections not only yield transparent proofs of the classical enumeration results, but also open the way to studying probabilistic and geometric properties of random maps, leading to scaling-limit theorems and the construction of the Brownian map [Le 13; Mie13].

The central focus of this thesis is precisely these bijections between maps and tree-like structures. Trees are among the most elementary combinatorial objects, and encoding maps through decorated trees reveals structural features that may be hidden in analytic methods. Following ideas of Bernardi, Albenque, Chapuy, and others [BF12; AP15; CD17], we distinguish between two families of bijections:

- Category (A): blossoming-tree bijections, in which a map is encoded by a spanning tree of the map decorated with additional information;
- Category (B): non-spanning-tree bijections, in which the encoding uses alternative tree-like structures such as labeled trees or mobiles.

Both families have been extended in recent years to more general classes of maps, including those embedded in higher-genus surfaces.

The aim of this thesis is to present a unified account of these bijections. While the constructions originate from different authors and were often developed independently, they share a number of common principles. This thesis:

- Collects a broad selection of bijections from the literature and presents them with a notation as consistent and unified as possible;
- Highlights the structural similarities and differences between various bijections;
- Proposes a unified scheme for each category, showing how many of the known constructions can fit into a common framework;

- Provides detailed proofs for selected central results, in particular the Cori-Vauquelin-Schaeffer bijection and the unified blossoming-tree scheme;
- Discusses applications of bijective methods to enumeration and to geometry.

The outline of this thesis is as follows.

Chapter 2 introduces the basic objects and terminology used throughout the thesis. We begin with directed and undirected graphs and then define planar maps as embeddings of graphs into the sphere, emphasizing the role of the cyclic order of edges around a vertex. We also recall properties of plane trees, including spanning trees, which will play a central role in later bijective constructions. Chapter 3 surveys a wide range of bijective constructions found in the literature. The bijections are divided into two categories as outlined above. For both categories, unified schemes are presented, and extensions to maps of higher genus are included. In Chapter 4, we provide detailed proofs of two central results to illustrate the mechanics of bijective methods in detail. First, we give a proof of the CVS bijection, following ideas of Chassaing, Schaeffer, and Chapuy, which demonstrates how quadrangulations can be encoded by well-labeled trees. Second, we present a proof of the generic blossoming tree scheme developed by Albenque and Poulalhon, which unifies earlier bijections in category (A). Finally, Chapter 5 discusses two major areas of application. Using the bijections presented earlier, we derive classical results such as the enumeration of rooted Eulerian maps and quadrangulations. We then turn to the probabilistic perspective, where bijections serve as a starting point for analyzing distances in random maps. In particular, we discuss how the CVS bijection has been used to prove that distances in random quadrangulations scale like $n^{1/4}$, and how this leads to the Brownian map as a universal scaling limit.

Preliminaries

This chapter collects most of the basic graph-theoretical notions used throughout the thesis. After defining directed and undirected graphs as mathematical objects and many of their properties, we continue with planar maps as proper embeddings of graphs in the sphere, together with many related concepts and some basic results. We then proceed with plane trees, recalling their structural properties, the notion of spanning trees, and some classical results. These notions form the common language for the bijections developed in the subsequent chapters.

2.1 Planar maps

We start with directed and undirected graphs and then turn to planar maps, which formalize the idea of drawing a graph in the plane or on the sphere in a way that fixes the cyclic order of edges around each vertex. This framework will be fundamental for our combinatorial encodings discussed later.

Definition 2.1.1: An undirected graph G = (V, E) is an object consisting of the set of vertices V = V(G) and the set of edges E = E(G), where each edge $e \in E$ is associated with an unordered pair $\{u,v\}$ of vertices $u,v\in V$. The association of edges and unordered pairs of vertices can be formalized by the mapping

$$\iota \colon \begin{cases} E \to \{\{u,v\} : u,v \in V\}, \\ e \mapsto \{u,v\} \end{cases}$$

called incidence relation.

Here we always assume V(G) and E(G) to be finite.

Definition 2.1.2: Let G = (V, E) be an undirected graph and ι be the corresponding incidence relation. An edge e is **incident** to vertices u and v if $\iota(e) = \{u, v\}$. In that case, u and v are the **endvertices** of e and the edge e is said to **connect/join** the two vertices. If we cut an edge e at its middle point, we get two half-edges, each is incident to its corresponding endvertex of e. We call two vertices u and v adjacent, if there exists an edge e with $\iota(e) = \{u, v\}$. We call an edge e a **loop** if $|\iota(e)| = 1$. Edges $e \neq e'$ are called **multi-edges** if $\iota(e) = \iota(e')$. An undirected graph without loops or multi-edges is called simple.

Figure 2.1 shows an example of an undirected graph with one loop and two multi-edges. The degree of a vertex is an important term in the study of graphs.



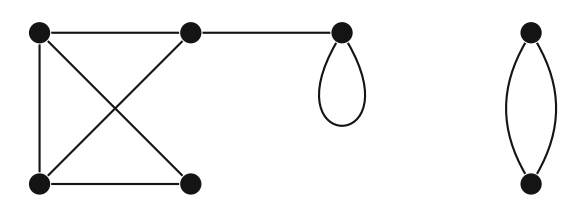


Figure 2.1: An undirected graph with multi-edges and one loop.

Definition 2.1.3: Let G = (V, E) be an undirected graph and $v \in V$. Let H(v) define the half-edges incident to v. We define the (vertex-)degree of v as

$$\deg_G(v) := |H(v)|.$$

A vertex of degree 0 is called **isolated**.

With this slight adaptation of the standard definition of the vertex-degree, we present a result also known as the Handshaking-Lemma.

Lemma 2.1.4: For an undirected graph G = (V, E) the following formula holds

$$\sum_{v \in V} deg_G(v) = 2 \cdot |E|.$$

Proof. Since each half-edge is incident to exactly one vertex, the left-hand side counts the total number of half-edges in the graph. Each edge consists of exactly two half-edges; thus, this number is $2 \cdot |E|$.

In many cases, we want to consider graphs that have a direction for each of the edges.

Definition 2.1.5: A directed graph G = (V, E) is also an object consisting of the set of vertices V = V(G) and the set of edges E = E(G), where each edge $e \in E$ is associated with an **ordered** pair (u,v) of vertices $u,v \in V$. The association of edges and ordered pairs of vertices can be formalized by the mapping

$$\overrightarrow{\iota} : \begin{cases} E \to V \times V, \\ e \mapsto (u, v) \end{cases}$$

also called incidence relation. For $e \in E$ and $\overrightarrow{\iota}(e) = (u,v)$ we also use the notation e=(u,v) and $e^-:=u,e^+:=v$. In this case, we call u the tail and v the head of e. The notation of Definition 2.1.2 can be adopted analogously.

The orientation of edges in a directed graph is usually illustrated by a little arrow, as can be seen in Figure 2.2.

Every directed graph naturally induces an underlying undirected graph by replacing each edge e associated with the ordered pair (u, v) by an edge e' associated with the unordered pair $\{u, v\}$.

Definition 2.1.6: Let G = (V, E) be a directed graph and $v \in V$. We define the **in-degree** and **out-degree** of v as

$$\deg_G^-(v) := |\{e \in E | \exists u \in V : \overrightarrow{\iota}(e) = (u, v)\}|,$$

$$\deg_G^+(v) := |\{e \in E | \exists w \in V : \overrightarrow{\iota}(e) = (v, w)\}|.$$

The **degree** of $v \in V$ is defined as $\deg_G(v) := \deg_G^-(v) + \deg_G^+(v)$.

Note that by definition the degree of a vertex v in a directed graph is exactly the degree of v in the underlying undirected graph.

Analogously to Lemma 2.1.4, we can state the Handshaking-Lemma for directed graphs.

Lemma 2.1.7: For a directed graph G = (V, E) the following formula holds

$$\sum_{v\in V} deg^-_G(v) = \sum_{v\in V} deg^+_G(v) = |E|.$$

In directed and undirected graphs, we want to consider various sequences of edges.

Definition 2.1.8: Let G = (V, E) be an undirected graph. A path of length k is a sequence of edges $p = e_1, e_2, \dots, e_k$ for which there exist distinct vertices $v_0 = u, v_1, \dots, v_k = v_0$ v, such that

$$\iota(e_i) = \{v_{i-1}, v_i\}, \text{ for } i = 1, \dots, k.$$

A directed path p is defined analogously, with edges satisfying

$$e_i = (v_{i-1}, v_i), \text{ for } i = 1, \dots, k$$

In both cases, we say that u, v are **connected** by the (directed) path and write len(p) = k. A graph G is called **connected** if each pair of vertices is connected. ¹ If we allow $v_0 = v_k$ and $k \ge 1$, the path is called a (directed) cycle.

Figure 2.2 illustrates a directed graph. It is disconnected as there exists an isolated vertex that is not connected to any of the other vertices. Apart from the loop, the graph contains exactly one (directed) cycle, which is highlighted in red (and dashed).

With the definition of a path, the notion of distance between two vertices follows very naturally.

Definition 2.1.9: Let G = (V, E) an undirected graph and $v_1, v_2 \in V$. The distance $d(v_1, v_2) := d_G(v_1, v_2)$ is defined as

$$d_G(v_1, v_2) := \inf\{\operatorname{len}(p)|p \text{ is a path in } G \text{ connecting } v_1 \text{ and } v_2\}.$$

By this definition, the distance between two vertices is ∞ if they are not connected. For a connected graph G, (G, d_G) can easily be shown to be a metric space.

We now introduce a special class of graphs that will be the basis for most of the upcoming considerations.



¹In the case of directed graphs, this only requires the underlying undirected graph to be connected, and is often called weakly connected.

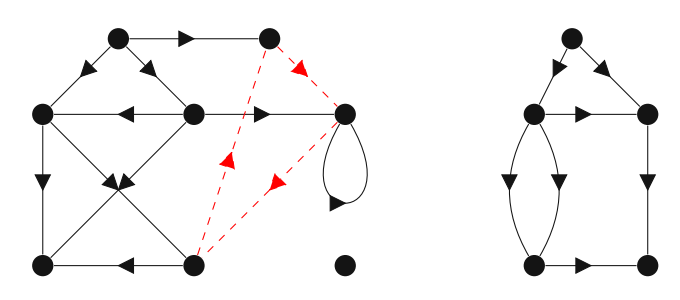


Figure 2.2: A disconnected directed graph with a directed cycle in red and dashed.

Definition 2.1.10: A tree is an undirected connected graph without a cycle.

The following classical characterizations of trees are standard and used repeatedly; we state them without proof.

Theorem 2.1.11: Let G be an undirected graph and n = |V(G)|. Then, the following statements are equivalent:

- 1. G is a tree (i.e., connected and acyclic).
- 2. G is connected and |E(G)| = n 1.
- 3. G is acyclic and |E(G)| = n 1.
- 4. For each pair $v, w \in V(G)$, there exists a unique path between v and w.
- 5. G is minimal connected (i.e., the removal of an edge disconnects G).
- 6. G is maximal acyclic (i.e., the addition of an edge creates a cycle).

Another important concept is that of bipartite graphs.

Definition 2.1.12: Let G = (V, E) be an undirected graph with a partition of the vertices in V into two subsets V_1 and V_2 . If for every edge e one endvertex is in V_1 and the other in V_2 , we call the graph **bipartite**.

We present a classical result which characterizes bipartite graphs.

Lemma 2.1.13: Let G be an undirected graph. G is bipartite if and only if it contains no cycle of odd length.

In this section, we have already shown some examples of graphs drawn in the plane. Since a given graph can usually be represented by many different drawings, it is natural to introduce the concept of planar maps as proper embeddings in the 2-sphere.

Definition 2.1.14: An **embedding** of an undirected graph G is an injective function ϕ from G into the 2-sphere. More explicitly, an embedding maps the vertices of G onto distinct points of \mathbb{S}^2 , and each edge of G onto a simple path on \mathbb{S}^2 connecting the images of its endpoints. An embedding is **proper** if distinct edges intersect only at their endpoints.

A planar map is a proper embedding of a connected graph G into the sphere \mathbb{S}^2 .

Later we will provide a generalized definition for maps on general surfaces (i.e., not only planar maps). Although most of the following definitions and results hold for maps on general surfaces, we will restrict ourselves to planar maps for now and explicitly indicate when a statement applies only in the planar case.

From now on, we will not distinguish between the vertices and edges of a graph and those of its embedded map.

Since an embedding determines the cyclical order of the edges around each vertex, we can define the following.

Definition 2.1.15: In a planar map, we define a **corner** c as a pair of consecutive halfedges around a vertex. The half-edge that appears first (or second) in clockwise order around the vertex is said to be on the left side (or on the right side) of the corner c. It is also possible to view corners as the angular sector between those two half-edges or as incidences between vertices and faces.

A rooted planar map is a planar map with a distinguished corner called the root **corner.** The oriented edge e_* that lies on the left side of the root corner and is oriented away from the associated vertex, is called the **root edge**. The vertex of the root corner is called the **root vertex**.

A rooted planar map is **pointed** if it has an additional distinguished vertex called pointed vertex. In this case, the map is called root-pointed if the pointed vertex and the root vertex coincide.

Planar maps are often not illustrated as embeddings in the 2-sphere, but rather by their representation in the plane. This representation can be obtained by choosing one face of the planar map as the infinite unbounded face in the plane. In a rooted planar map, it is common to mark either the root corner or the oriented root edge in an illustration.

Definition 2.1.16: Let M be a planar map. A face is a connected component of $\mathbb{S}^2 \setminus M$. The faces of a map M are denoted by F(M). The **degree** $\deg_M(f)$ of a face f is the number of incident corners.

Note that one would actually need Jordan's curve theorem in order to thoroughly define the faces of a planar map. We omit these details here and proceed with our intuitive definition.

The following result is analogous to the Handshaking-Lemma.

Lemma 2.1.17: For every planar map M the following formula holds

$$\sum_{f \in F(M)} deg_M(f) = 2 \cdot |E(M)|. \tag{2.1}$$

Another well-known result, called Euler's (polyhedron) formula for planar maps, and its inductive proof on the number of edges can be found in [Die17] (Theorem 4.2.9.).

Theorem 2.1.18: Let M be a planar map. Then

$$|V(M)| - |E(M)| + |F(M)| = 2.$$

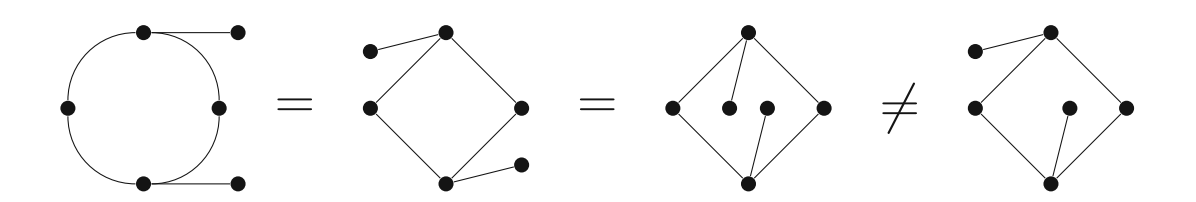


Figure 2.3: Plane representation of planar maps $M_1 = M_2 = M_3 \neq M_4$.

It is important to keep in mind that we always work with maps seen up to "deformation", or more precisely.

Definition 2.1.19: Two planar maps M and M' are called **isomorphic** if there exists an orientation-preserving homeomorphism h on \mathbb{S}^2 such that V(M) = h(V(M')) and E(M) =h(E(M')). The mapping h is called a (map-)isomorphism. Let the maps M and M' be rooted with root edges e_* and e'_* , then they are **isomorphic** if there exists a mapisomorphism h such that $h(e_*) = e'_*$.

Note that a map-isomorphism preserves not only the incidence relation between vertices and edges but also the incidence relation between edges and faces. Figure 2.3 shows the plane representation of four maps M_1, \ldots, M_4 . Note that all maps are proper embeddings of the same underlying graph, but only $M_1 = M_2 = M_3$ are the same planar map. The first equality is easy to see because both maps are deformations of each other in the plane. For the second equality, one needs to realize that the two maps M_2 and M_3 are different plane representations of the same planar map with different faces chosen as the infinite outer face. The planar map M_4 has two faces of degree 6 and therefore can not be equal to the other planar maps that have one face of degree 4 and one face of degree 8.

The identification of maps up to isomorphisms is necessary for the enumeration of these combinatorial structures.

Definition 2.1.20: The isometry classes of all planar maps with $n \geq 1$ edges are denoted by \mathcal{M}_n and the class of all planar maps by $\mathcal{M} = \bigcup_{n>1} \mathcal{M}_n$.

Definition 2.1.21: A map is called Eulerian if all its vertices have even degree² and m-regular if all its vertices have degree m. We call a map even if all its faces have even degrees and m-angulation if all its faces have degree m. For the special cases m=3,4,we use the terms **triangulation** and **quadrangulation**.

Lemma 2.1.22: In the planar case, all even maps are bipartite. Thus, all planar quadrangulations are bipartite.

Proof. Let M be an even planar map. We assume M is not bipartite; therefore, it contains a cycle c of odd length according to Lemma 2.1.13. The cycle c partitions the rest of

²Usually, the property of being Eulerian is defined by the existence of an Euler tour (a closed walk in a graph that traverses every edge of the graph exactly once). It was shown by Euler in the 18th century that for a connected graph, this is equivalent to the definition of even vertex-degrees; hence we use this definition for our purposes.

the sphere $\mathbb{S}^2 \setminus c$ into two non-empty connected components P_1 and P_2 . Let M' be the map obtained by only considering the cycle c and the vertices and edges contained in P_1 . Now, P_2 is a face of M' bounded by c and since c is of odd length, P_2 has an odd degree. According to Formula (2.1), one of the other faces of M' must also have an odd degree. This produces a contradiction, since the other faces of M' are also faces of the original even map M.

Note that this proof does not generalize to the case of general maps. A cycle does not necessarily produce two non-empty connected components on a surface of higher genus (e.g., the surface of a torus). For general maps, only the other implication holds true; a map is even if it is bipartite.

Definition 2.1.23: Let M be a map with a partition of the faces F into two non-empty subsets F_1 and F_2 . If each edge e is incident to one face in F_1 and one in F_2 , M is said to be bicolorable.

There exist several interesting constructions for planar maps; a few of them are introduced here.

Definition 2.1.24: Let M be a planar map. Its dual M^* is the map with vertex set V^* obtained by placing a vertex f^* in each face f of M, and with edge set E^* obtained by drawing an edge e^* across each edge e of M connecting the vertices corresponding to the incident faces.

Definition 2.1.25: Let G be an undirected graph. A subgraph T is called a spanning **tree** of G if T is a tree and V(T) = V(G).

Theorem 2.1.26: Let M be a planar map with dual M^* . For each edge $e \in E(M)$, denote by $e^* \in E(M^*)$ its dual edge. Then the edges $T \subseteq E(M)$ form a spanning tree of M if and only if

$$T^* := \{e^* : e \notin E(T)\}$$

form a spanning tree of M^* .

Proof. Let n = |V(M)|, m = |E(M)|, f = |F(M)|. By Euler's formula, we have n - m + f = |F(M)|2. Let T be a spanning tree of M, then |E(T)| = n - 1, hence

$$|T^*| = m - (n-1) = f - 1 = |V(G^*)| - 1.$$

Thus, T^* is a spanning tree if it is a tree. Assume that T^* contains a cycle. We take two arbitrary vertices $v_1, v_2 \in V(M) = V(T)$ that lie on different sides of the cycle. These two vertices cannot be connected by a path in T since this path would need to contain an edge dual to an edge of the cycle. This is in contradiction to T being connected.

Using very similar arguments, it can be shown that T^* is connected since T does not contain a cycle. The other implication of the statement can be shown in the same way by switching the roles of M and M^* and using the fact that $(M^*)^* = M$.



With the help of dual maps, we can show another equivalence of definitions in the planar case.

Lemma 2.1.27: In the planar case, all Eulerian maps are bicolorable.

Proof. This is in fact a direct consequence of Lemma 2.1.22. Let M be a planar Eulerian map, then its dual M^* is a planar even map, since the property of even face degrees translates directly into even vertex degrees in the dual case. By Lemma 2.1.22, M^* is bipartite. If a dual map is bipartite, its original map M must, by definition, be bicolorable.

Definition 2.1.28: A bipartite map with partition $V_1 \cup V_2$ is called **vertex-bicolored** if the vertices of V_1 are colored black and those of V_2 white. Given a planar map M, its vertex-bicolored incidence map (or quadrangulation) Q(M) is the map with vertex set $V \cup V^*$, vertices of V colored black and vertices of V^* colored white. The edge set is created as follows: For each corner c around a vertex v of the original map M, draw an edge between the vertex $v \in V$ and the vertex $f^* \in V^*$, where f is incident to the corner c.

Remark 2.1.29: The mapping Q is a bijection from planar maps with n edges to vertexbicolored planar quadrangulations with n faces. Given such a quadrangulation, the corresponding map can be recovered by drawing, in each face, a diagonal between the two black corners of that face. The set of black vertices together with these diagonals, yields the original map. ³

The plane representation of a planar map M with 4 edges and its corresponding quadrangulation Q(M) with 4 faces is shown in Figure 2.4. In the left subfigure, the original map M is still depicted with dashed edges.

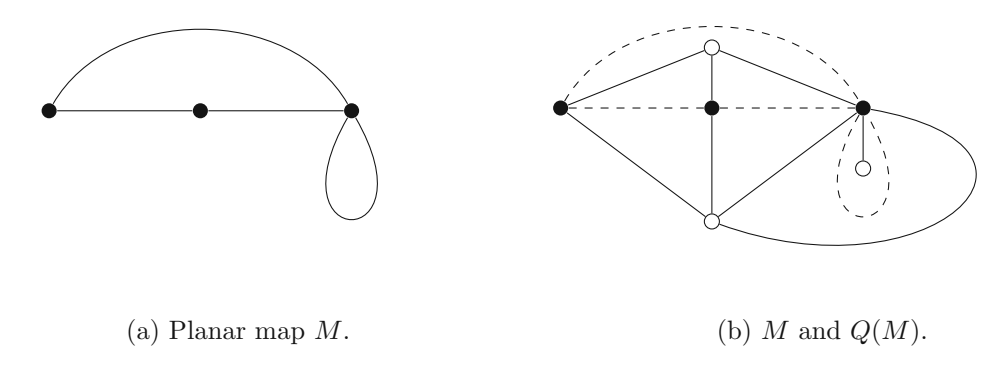


Figure 2.4: A planar map and its quadrangulation.

Definition 2.1.30: Let M be a planar map. We construct a new map by drawing a vertex e^* in the middle of each edge e of M. For each corner of the map M and its incident edges e_1 and e_2 , we draw an edge between the vertices e_1^* and e_2^* . This construction yields the medial map of the map M.



 $^{^3{\}rm This}$ also holds for general surfaces (see [CD17]).

A planar map M with 6 edges and its medial map with 12 edges are illustrated in Figure 2.5. In Subfigure 2.5b, the original map M is still depicted with white vertices and dashed edges to show the connection between both maps.



Figure 2.5: M and the medial map construction.

In fact, there is a relation between the number of edges, and one can even show how the construction can be reversed. For now, we focus on rooted planar map. Let c be the root corner (with the root edge e_0 to its left). The root corner of the medial map is then defined as the corner that contains e_0 .

Since the medial map has an edge for each corner of the original map, a planar map with n edges yields a medial map with 2n edges. Furthermore, considering any vertex e^* of the medial graph and one of the two half-edges of the edge e, the half-edge is either incident to two different corners or incident twice to the same corner. Thus, the half-edge produces either two edges or a loop, in both cases contributing 2 to the degree of the vertex e^* . This shows that each vertex has degree 4.

The reverse construction is given as follows: consider a rooted 4-regular map with 2nedges. Since the map is Eulerian, its dual graph is bipartite, allowing us to color the faces of the map in two colors c_1 and c_2 ; let c_1 be the color of the face f_0 that contains the root corner. We construct a map M with a vertex f^* for each face f of color c_1 . Whenever two faces f_1 and f_2 (not necessarily distinct) are incident to different corners of a shared vertex, an edge is added between f_1^* and f_2^* . There is one specific edge, whose creation includes the root corner (and the vertex f_0^*). This edge is chosen as the root edge of M oriented away from f_0^* . The so constructed rooted planar map M has n edges, and it can be checked that these constructions are inverse.

Lemma 2.1.31: The medial map construction is a bijection between rooted planar maps with n edges and rooted 4-regular planar maps with 2n edges.

Later, we will apply this lemma to a certain class of planar maps which can be interpreted as a subclass of rooted planar maps.

Definition 2.1.32: A plane map (also called a face-rooted map) is a proper embedding of a connected graph in the plane. The unique unbounded face is called the **outer face** or root face, every other face is called inner face.



The outer degree of a plane map is the degree of the outer face. Vertices, edges and corners are called **outer** if they are incident to the outer face and **inner** otherwise.

Plane maps can also be defined as planar maps with a marked root face; if we already have a rooted planar map, we can interpret it as a plane map and take the face incident to the root corner as root face. When illustrated in the plane, the root face is taken as the unbounded outer face.

We emphasize that plane maps and planar maps are a very similar yet different concept and must not be confused. It is interesting to refer to Figure 2.3 again and mention that M_2 and M_3 are not equal when they are interpreted as plane maps. This is obvious from the fact that they have different outer degrees.

2.2 Plane trees

Plane trees are among the most fundamental combinatorial objects and are frequently used for the purpose of map enumeration. In this section, we recall their definitions and basic properties, setting the stage for their role in bijections with planar maps.

Definition 2.2.1: A **(rooted) plane tree** is a (rooted) planar map without cycle (and thus with only one face). The vertices of a tree are also called **nodes**. The nodes with degree 1 are called leaves and the nodes with higher degree are called internal nodes. By \mathcal{P} and \mathcal{P}_n we denote the class of rooted plane trees and the subset of rooted plane trees with n edges, respectively.

Rooted plane trees can also be defined recursively as a root node to which is attached a (possibly empty) sequence of rooted plane trees. This leads to the combinatorial equation

$$\mathcal{P} = \{\bullet\} \times \mathcal{P}^*, \tag{2.2}$$

where \bullet denotes the root node and \mathcal{P}^* denotes the sequence class of the class \mathcal{P} defined as

$$\mathcal{P}^* := \{\epsilon\} + \mathcal{P} + (\mathcal{P} \times \mathcal{P}) + (\mathcal{P} \times \mathcal{P} \times \mathcal{P}) + \cdots$$

Using the combinatorial equation (2.2) and basic methods of analytic combinatorics, the ordinary generating function (OGF) of rooted plane trees is given by

$$P(z) = \frac{z}{1 - P(z)}.$$

In [FS09], a detailed introduction to combinatorial classes and generating functions can be found. In the book, they also solve the functional equation for the coefficients of the OGF and show the following well-known theorem.

Theorem 2.2.2 ([FS09], I.5.1): The number of rooted plane trees with n edges is given by

$$|\mathcal{P}_n| = C_n = \frac{1}{n+1} \binom{2n}{n},\tag{2.3}$$

where C_n denotes the n-th Catalan number.

Rooted plane trees are usually depicted in a canonical form, where the root corner is at the top. As an example, two different illustrations of the same plane tree are shown in Figure 2.6. This rooted plane tree is rooted at an internal node and is therefore different from a specific class of rooted plane trees that we define in the following.

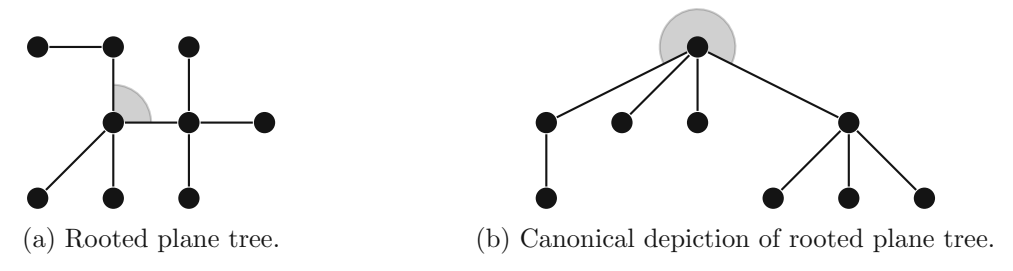


Figure 2.6: The same rooted plane tree.

Definition 2.2.3: A planted plane tree is a plane tree rooted at the (unique) corner of a leaf.

Note that the definition of planted plane trees is almost identical to the definition of rooted plane trees. In fact, for $n \geq 1$, each planted plane tree with n edges can be converted to a rooted plane tree with n-1 edges by removing the root leaf and its incident edge and adding a new root corner instead, and vice versa. Thus, according to Formula (2.3), the number of planted plane trees with n edges is given by C_{n-1} .

Definition 2.2.4: A rooted plane tree is **labeled** if all its nodes are additionally given integer labels.

It is **embedded** if the labels of two adjacent nodes differ by at most 1 and the label of the root node is 1. By \mathcal{E} and \mathcal{E}_n , we denote the set of embedded rooted plane trees and the subset of embedded rooted plane trees with n edges, respectively.

If in addition all nodes have positive labels, the tree is called **well-labeled**.

Consider a given embedded plane tree $T \in \mathcal{E}_n$. For each of the n edges, we have 3 different choices for the relation between the labels of the two corresponding endvertices (being equal or differing by one). Together with Formula (2.3) for the number of rooted plane trees, this gives us

$$|\mathcal{E}_n| = 3^n \cdot |\mathcal{P}_n| = \frac{3^n}{n+1} \binom{2n}{n}.$$

We have already used the notion of the clockwise order of edges around a given vertex that exists for all vertices in a given map. For a face-rooted map, we can additionally define a clockwise tour around the map, which is very natural considering the corresponding embedding in the plane.

Definition 2.2.5: Let M be a face-rooted planar map with m outer corners. We define the clockwise tour around the map as the cyclic sequence of outer corners and outer edges

$$\left(c^{(0)}, e^{(0)}c^{(1)}, e^{(1)}, \dots, c^{(m-1)}, e^{(m-1)}\right),$$

such that for each $0 \le i \le 2n-1$, the edge $e^{(i-1)}$ lies on the left side and the edge $e^{(i)}$ on the right side of the corner $c^{(i)}$.⁴

If the map is corner-rooted, the clockwise tour becomes an acyclic sequence starting at the root corner.

Since a plane tree $T \in \mathcal{P}_n$ has only one face, each corner is an outer corner. Thus, the clockwise tour around the tree contains each of the 2n corners, and each of the n edges twice.

⁴For i = 0, the edge $e^{(-1)}$ is defined to be the edge $e^{(n-1)}$ due to the cyclic nature of the tour.

Overview of bijections between maps and tree-like structures

In this chapter, we present a non-exhaustive overview of different bijections between maps and tree-like structures. We try to cover the most important advances in research in recent years and shed light on the differences and connections between these different approaches.

A strategy of clustering the bijections into two different families of constructions could be made similarly to [BF12]. The bijections can be divided into two categories: (A) bijections in which the decorated tree is a spanning tree of the map, and (B) bijections in which the decorated tree is no longer a spanning tree of the corresponding map. These trees are bicolored and called mobiles in various sources.

3.1 Bijections of category (A)

In this section, we explore a fundamental class of bijections between combinatorial objects; we will call those bijections of category (A). These bijections serve as a powerful tool to translate complex problems about maps on surfaces into more tractable structures such as decorated trees or unicellular maps with additional data. Originating from seminal work in planar map theory, these bijections have been extended and generalized to surfaces of higher genus and to both orientable and non-orientable settings.

The core idea behind bijections of category (A) lies in encoding maps through wellstructured unicellular blossoming maps, where combinatorial constraints translate into conditions on stems, labels, and orientations. This encoding not only enables enumerative formulas but also provides insight into the metric and geometric properties of maps via the study of the simpler underlying structures.

In particular, this section covers bijections between planar maps and blossoming trees, as well as their Eulerian and triangular variants, and the higher-genus generalizations developed in recent works.

3.1.1 Schaeffer's construction for Eulerian maps

In this subsection, we introduce the concept of a class of decorated trees called blossoming trees via the bijection between Eulerian planar maps with a prescribed sequence of vertex degrees and blossoming trees, as described in [Sch97]. Note that [Sch97] uses the notion of an Eulerian tree. Since we want to highlight their role in the context of blossoming trees, we will slightly modify them and use the notion of Eulerian blossoming trees instead.

Definition 3.1.1: A **blossoming map** is a face-rooted map, in which each outer corner can carry a sequence of opening or closing stems.

A blossoming tree is a blossoming map based on a plane tree. A blossoming tree with d_i vertices of degree 2i is called **Eulerian** if each vertex of degree 2i carries i-1 opening stems.

The cyclic contour word of a blossoming map is the word on $\{e,b,\overline{b}\}$, which encodes the cyclic order of edges and stems along the clockwise tour around the map, where eencodes an edge, b encodes an opening stem and \bar{b} encodes a closing stem.

A local closure of a blossoming map is a substitution of a factor be^*b by the letter e in its contour word, where e^* denotes any (possibly empty) sequence of e.

A local closure corresponds very naturally to replacing an opening stem and a later (in the clockwise tour around the map) closing stem by a single new edge in the map. This new edge is called a **closure edge**.

The opening and closing stems are usually depicted as little outgoing and ingoing arrows. The left side of Figure 3.1 shows an Eulerian blossoming tree with 3 opening and 5 closing stems. The cyclic contour word of this tree is given by $beb\bar{b}e\bar{b}e\bar{b}e\bar{b}e\bar{b}e\bar{b}e$.

For our upcoming considerations, we introduce a basic combinatorial result.

Lemma 3.1.2: Let n, k be positive integers. The number of k-tuples (n_1, \ldots, n_k) with $\sum_{i=1}^{k} n_i = n \text{ is given by}$

$$\binom{n+k-1}{k-1}$$
.

Proof. The problem of enumerating those k-tuples is equivalent to the problem of counting the possibilities of placing n objects into k bins. The bins are distinguished but the nobjects are not.

Each of these possibilities can be encoded by an arrangement of stars and bars, where each of the n objects is represented by a star and two adjacent bins are separated by a bar. Each encoding consists of n stars and k-1 separating bars and is uniquely determined by the position of the k-1 bars. Thus, the problem is reduced to choosing k-1 out of n+k-1 possible positions.

There is an interesting connection between Eulerian blossoming trees and plane trees. An Eulerian blossoming tree with d_i vertices of degree 2i can be obtained from a plane tree in which each corresponding vertex has degree i + 1. This correspondence comes from replacing each leaf and its incident edge by a closing stem, and adding i-1 opening stems to each internal vertex of degree i + 1. By Lemma 3.1.2, there are $\binom{2i-1}{i}$ possible ways. If one starts with a plane tree with k leaves and n edges, the resulting Eulerian blossoming tree has k closing stems and n-k edges.

In Figure 3.1 we show an example of an Eulerian blossoming tree and its underlying

We continue with a lemma on the number of leaves in a plane tree, which will be used in the subsequent analysis.

Lemma 3.1.3: Let T be a plane tree with d_i vertices of degree i+1 for $i \geq 1$. Then, the number k of leaves in T is given by

$$k = 2 + \sum_{i \ge 2} (i - 1)d_i. \tag{3.1}$$

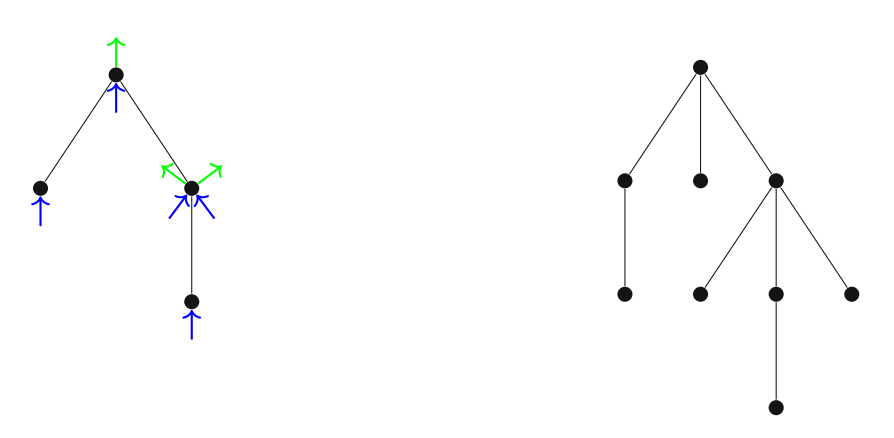


Figure 3.1: Eulerian blossoming tree and its underlying plane tree.

Proof. We prove the result by induction on the number of edges. For the base case, consider a plane tree consisting of two nodes connected by a single edge. Both nodes have degree 1 (so $d_i = 0$ for $i \ge 2$), and Formula (3.1) yields k = 2, as required.

Let T be a plane tree with d_i vertices of degree i+1 and \tilde{T} be the plane tree with \tilde{d}_i vertices of degree i + 1 after cutting off a leaf and the connecting edge. If the leaf was attached to a node of degree j + 1 > 2, then the number of leaves and the sum are both reduced by 1. If the leaf was attached to a node v of degree j + 1 = 2, then the number of leaves and the sum both remain the same, since the node v is a new leaf and since $d_i = d_i$ for all $i \geq 2$.

Lemma 3.1.4: An Eulerian blossoming tree has exactly two more closing stems than opening stems. This property is invariant under any sequence of local closure operations.

Proof. Consider an Eulerian blossoming tree with d_i vertices of degree 2i. By Lemma 3.1.3, the number of leaves of the underlying plane tree with d_i vertices of degree i+1 is given by

$$k = 2 + \sum_{i \ge 2} (i - 1)d_i,$$

which equals the number of closing stems of the Eulerian blossoming tree. Since i-1opening stems are added to each of the d_i nodes of degree i+1, the number of opening stems is given by $\sum_{i\geq 2} (i-1)d_i$, so the difference is exactly 2.

A local closure removes one opening stem and one closing stem and, therefore, does not affect this property.

If two different local closures are possible on a given blossoming map, the order of performing them does not change the result. As long as the letter b appears in the contour word, we can find a cyclic permutation containing a factor $be^*\bar{b}$ and thus yielding a local closure. Hence, iterating closures in any order eventually produces a unique map, which justifies the following definition.

Definition 3.1.5: The complete closure \overline{M} of a blossoming map M is the object obtained by iterating all possible local closures until no opening stems remain.

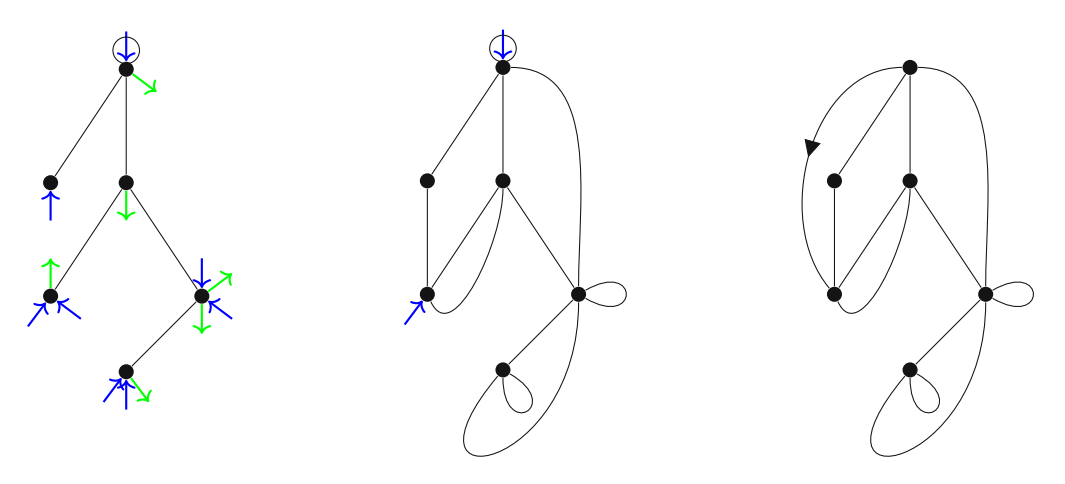
An example of an Eulerian blossoming tree and its complete closure is shown in Figure 3.2.

According to Lemma 3.1.4, the complete closure of an Eulerian blossoming tree contains no more opening stems and exactly two unmatched closing stems. These two closing stems will play a central role in the analysis of Eulerian blossoming trees.

Definition 3.1.6: An Eulerian blossoming tree is called **marked** if one of the closing stems is marked. In illustrations of a marked Eulerian blossoming tree, the marked closing stem is indicated by a small circle around it. Two marked Eulerian blossoming trees are called **conjugate** if one can be obtained from the other by changing which closing stem is marked.

A marked Eulerian blossoming tree is called balanced if its marked stem is one of the two unmatched closing stems in the complete closure.

The complete closure implies a mapping Φ from balanced Eulerian blossoming trees to another class of maps. Given the complete closure of a balanced Eulerian blossoming tree, we insert a directed root edge from the marked closing stem to the second unmatched closing stem. The resulting rooted Eulerian map has the same distribution of vertex degrees as the original blossoming tree. This final step can also be seen in Figure 3.2.



- (a) Eulerian blossoming tree.
- (b) The complete closure.
- (c) Eulerian map after final step.

Figure 3.2: The mapping Φ illustrated in two steps.

To illustrate why this mapping Φ is a bijection, we briefly sketch the construction of its

Algorithm 1 operates simultaneously on the contour word and on the corresponding (blossoming) map.

The exponent m-1 in e^{m-1} ensures that the updated cyclic contour word corresponds exactly to the blossoming map, in which the former marked edge is replaced by an opening stem and a closing stem.

We state the main theorem of this subsection and refer to [Sch97] for the proof.



Algorithm 1 Opening algorithm for rooted Eulerian maps Ψ

```
Require: M rooted Eulerian planar map, c the cyclic contour word of M
 1: e_0 \leftarrow the root edge
 2: while M is not a tree do
        f \leftarrow the inner face incident to e_0
        m \leftarrow \deg(f)
 4:
        e_1 \leftarrow e_0
        e_0 \leftarrow \text{the edge after } e_1 \text{ in } c
 6:
        if e_1 is not a bridge then
 7:
            if e_1 is the root edge then
 8:
                update c by substituting the letter e corresponding to e_1 by \bar{b}e^{m-1}\bar{b}
 9:
10:
                 update c by substituting the letter e corresponding to e_1 by be^{m-1}\bar{b}
11:
12:
            end if
            update the map M accordingly
13:
14:
        end if
15: end while
16: return blossoming tree M
```

Theorem 3.1.7: The mapping Φ is a bijection from balanced Eulerian blossoming trees with d_i vertices of degree 2i, k closing stems and n-k edges onto rooted Eulerian planar maps with d_i vertices of degree 2i, e = n - 1 edges, and v = n - k + 1 vertices.

The opening algorithm Ψ is its inverse.

This bijection will be applied in Section 5.1 to derive an enumeration formula for rooted Eulerian planar maps.

3.1.2 Triangulations

There exists a bijection between simple rooted triangulations (no loops or multi-edges) and a certain class of blossoming trees. The bijection is presented in ([PS06]).

Definition 3.1.8: A triangulation is of size n if it has 2n faces. By \mathcal{T}_n we denote the set of rooted simple triangulations of size n.

By Formula 2.1, a triangulation of size n has 3n edges. Applying Euler's formula then yields that the number of vertices is given by n+2.

There are exactly three different rooted simple triangulations of size 3; they are depicted in Figure 3.3. Observe that they differ only in the choice of the root edge. For larger values of n, two triangulations may also differ in the structure of their underlying planar map.

Aiming for a bijection onto rooted simple triangulations, in this subsection we introduce a variation of blossoming trees that differs slightly from the notation used in [PS06], but is closer to our notation used throughout this section.

Definition 3.1.9: A blossoming tree in which each node carries exactly two opening stems and no closing stem is called **triangular**. By $\mathcal{B}_n^{\triangle}$, we denote the set of triangular blossoming trees with n nodes.



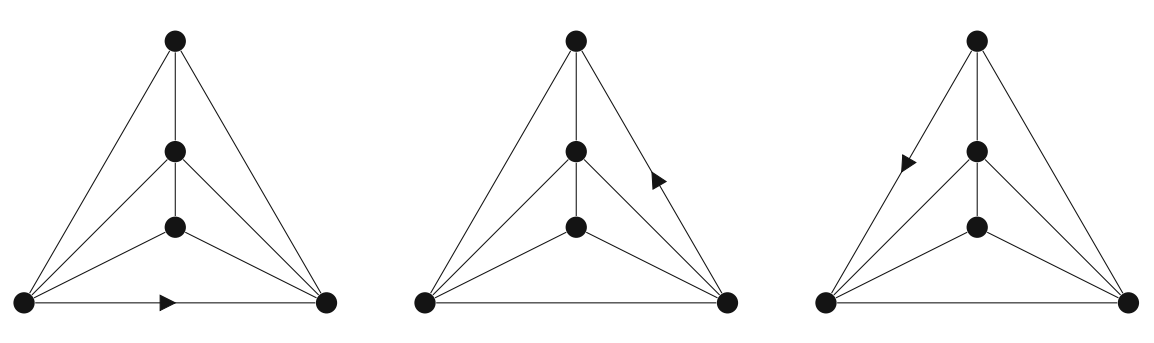


Figure 3.3: The 3 elements of \mathcal{T}_3 .

A (triangular) local closure of a blossoming map is the operation of substituting a factor bee by the letter e in its contour word. For a triangular blossoming tree T, the partial closure T is the result of the exhaustive recursive application of local closures.

We want to emphasize that the triangular local closure for blossoming maps differs from the general local closure for blossoming maps, although the underlying idea is conceptually very similar.

The triangular local closure can be interpreted as the substitution of an opening stem by an edge between the corresponding node and the next node in clockwise order so that a new triangular face is created.

The only two possible triangular local closures of a given triangular blossoming tree, and hence its partial closure, are illustrated in Figure 3.4. We ignore the circle around the one opening stem for now.

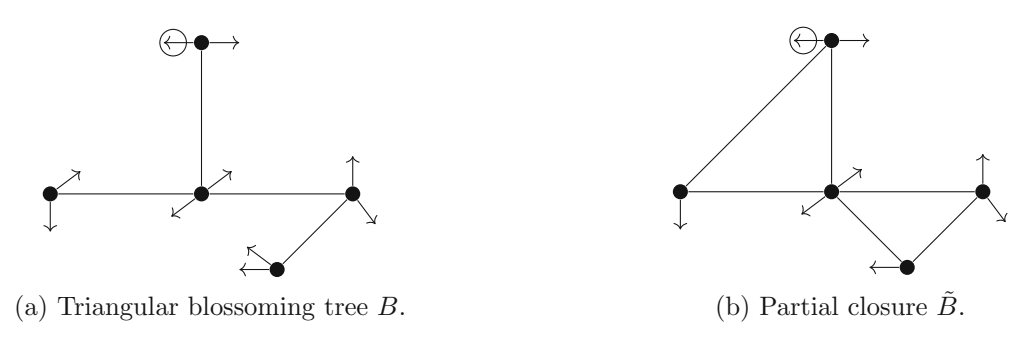


Figure 3.4: The effect of two local closures.

By definition, a triangular blossoming tree in $\mathcal{B}_n^{\triangle}$ has 2n opening stems and n-1 edges. Therefore, the letter b appears 2n times in the contour word and the letter e appears 2n-2times, because each of the n-1 edges is encountered exactly twice in a tour around the tree. By performing a local closure, the number of both quantities is effectively reduced by one and the difference between opening stems and edges remains 2. The partial closure cannot have two consecutive edges; otherwise, these edges together with one of the opening stems left would allow for another local closure. Thus, the resulting contour word is an alternating sequence of the letters b and e with the occurrence of two distinct positions in the word where two consecutive b's appear. The nodes corresponding to these places in the contour word, which carry both of their original opening stems, are called v_0 and v'_0 . The resulting contour word can be written as

$$\underbrace{(be)^{+}b}_{\text{I. part}}\underbrace{(be)^{+}b}_{\text{II. part}}$$
(3.2)

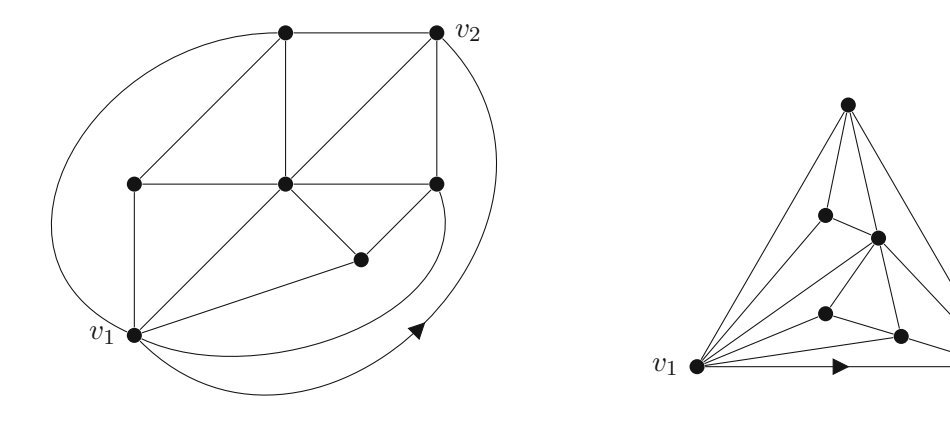
where $(be)^+$ denotes a non-empty sequence of be of any length. In the example of Figure 3.4, the resulting contour word of \tilde{B} can be written as $(be)^4b(be)^2b$.

Definition 3.1.10: A triangular blossoming tree is called **marked** if one of the opening stems is marked; it is called **balanced** if the last b of either the I. or II. part of the contour word encodes the marked opening stem. In illustrations of a marked triangular blossoming tree, the marked opening stem is highlighted by a small circle around it.

In a balanced triangular blossoming tree, the marked opening stem belongs, by definition, to either v_0 or v'_0 and comes before the other opening stem of that node in clockwise order.

Definition 3.1.11: Let $B \in \mathcal{B}_n^{\triangle}$ be a balanced triangular blossoming tree and \tilde{B} its partial closure with its contour word denoted as in (3.2) such that the marked opening stem belongs to the I. part. The **complete closure** of B is obtained from B by first adding two new nodes v_1 and v_2 , and replacing all opening stems of the I. part with an edge to v_1 and all opening stems of the II. part with an edge to v_2 . Finally, a directed root edge $e=(v_1,v_2)$ is added.

Figure 3.5a finalizes the complete closure that was started with the partial closure in Figure 3.4. Figure 3.5b shows the same map in an embedding that more clearly reveals its structure as a triangulation.



(a) Complete closure.

(b) Triangular structure.

Figure 3.5: Two embeddings of the complete closure.



It is straightforward to verify that the complete closure produces a triangulation with n+2vertices and thus of size n. However, it is not immediately obvious that the triangulation is simple, i.e., that it does not contain multiple edges. The proof can be found in Section 3.1 of [PS06].

The complete closure suggests a bijection between the set $\mathcal{B}_n^{\triangle}$ of balanced triangular blossoming trees with n nodes and the set \mathcal{T}_n of simple triangulations of size n.

To describe the inverse construction, we first define the notion of an orientation of a map.

Definition 3.1.12: An **orientation** of a planar map is the assignment of a direction for each edge. A planar map endowed with an orientation can be interpreted as the embedding of a directed graph, and from now on we will also adopt the notations of the associated directed graph for an oriented planar map. Let M be a planar map, V the set of vertices, and $\alpha:V\to\mathbb{N}$ a function that associates a natural number to each vertex of the map. An α -orientation is an orientation of M such that

$$\forall v \in V, \deg_M^-(v) = \alpha(v).$$

If such an orientation exists, α is said to be **feasible** on the map M.

We will work with orientations in more detail in Subsection 3.1.3. For the moment, we require this definition only to introduce the inverse construction.

Let $T \in \mathcal{T}_n$ be a rooted simple triangulation with outer vertices v_0, v_1, v_2 and root edge (v_1, v_2) . We equip T with the α -orientation corresponding to the function $\alpha(v) = 1$ for each outer vertex and $\alpha(v) = 3$ for each inner vertex, which contains no counterclockwise cycles.¹

We apply the following opening Algorithm 2 to a triangulation $T \in \mathcal{T}_n$:

The first two parts of Figure 3.6 show the steps before the while-loop of the opening algorithm applied to the triangulation obtained in Figure 3.5. In the figure, the current edge e (resp. the opening stem e chosen at the beginning of the algorithm) is represented in dashed lines. We highlight all the marked edges in red to keep track of when we exit the while-loop. This final configuration before exiting the loop is shown in the last subfigure of Figure 3.6. The resulting map consists of the two isolated vertices v_1 and v_2 , and the connected component containing v_0 . If we additionally mark the opening stem o_1 , we eventually obtain the original triangular blossoming tree of Figure 3.4.

We do not show here the correctness of this algorithm nor prove that this opening algorithm is the inverse of the complete closing. However, we recall the following key result from [PS06].

Theorem 3.1.13 ([PS06], Proposition 2.7): The opening algorithm returns a spanning tree of $T \setminus \{v_1, v_2\}$. The tree is the unique balanced triangular blossoming tree whose complete closure produces the triangulation T. Hence, the complete closure is a bijection between the set $\mathcal{B}_n^{\triangle}$ of balanced triangular blossoming trees with n nodes and the set \mathcal{T}_n of rooted simple triangulations of size n. Its inverse is given by the opening algorithm.

¹We will show later that such an orientation always exists and is unique.

²Here, $T \setminus \{v_1, v_2\}$ denotes the triangulation obtained by removing the two outer vertices v_1 and v_2 along with their incident edges.

Algorithm 2 Opening algorithm for triangulations

Require: $T \in \mathcal{T}_n$

Ensure: T is endowed with a minimal orientation

1: delete the root edge (v_1, v_2) and replace the edges (v_0, v_1) and (v_0, v_2) with opening stems attached to v_0 , denoted o_1 and o_2

```
2: e \leftarrow o_2, v \leftarrow v_0
\exists: while \exists unmarked edge do
        e' \leftarrow \{v, u\} the edge following e in clockwise direction
4:
        if e' is unmarked and directed towards v then
5:
             substitute e' by an opening stem attached to v
6:
        else
7:
             \max e'
8:
             e \leftarrow e', v \leftarrow u
9:
        end if
10:
11: end while
```

12: **return** connected component of v_0 with the marked opening stem o_1

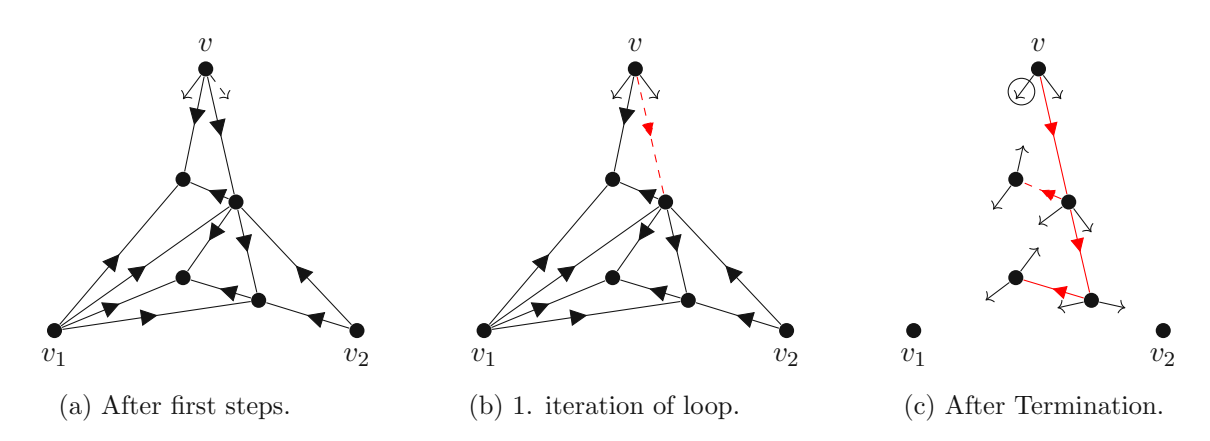


Figure 3.6: Opening algorithm for triangulations.

We will use this bijection in Subsection 5.1.2 to give an explicit formula for the number of rooted simple triangulations of size n.

3.1.3 Unified bijective scheme

In [AP15], the authors present a generic bijective scheme that unifies and generalizes previous bijections between planar maps and blossoming trees. This framework relies on orienting the map in a suitable way and produces a bijection between the map and a spanning tree decorated with additional structure, called a blossoming tree. Several known constructions, such as those described in Subsection 3.1.1, can be recovered as special cases of this scheme.

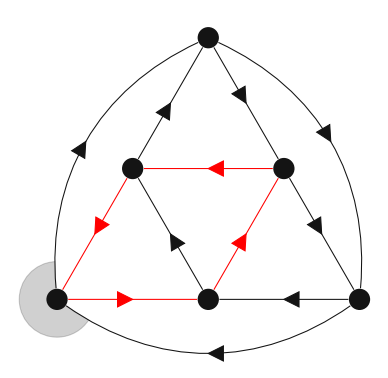
The paper presents a new bijective scheme, relying on an orientation of a map, between the map and a spanning tree of the map with some decorations, called blossoming tree.

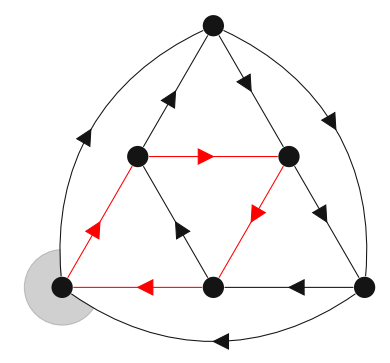
Next, we define an extension of plane maps that will be used throughout the rest of Section 3.1.

We begin by recalling some basic notions about orientations of planar maps.

Definition 3.1.14: An orientation of a map is called **accessible from** v if for every vertex $w \in V$ there exists a directed path from the root vertex to v. If the map has a root vertex v_0 , we call the orientation accessible if it is accessible from v_0 .³ For maps with a root face, we can define **clockwise** (resp. **counterclockwise**) **cycles** as directed cycles that have the outer face on their left (resp. right) when traversed according to the edge directions. An orientation without counterclockwise cycles is called **minimal**. The operation of reversing all edges of a given oriented cycle is called a flip.

In Figure 3.7, we can see the plane representation of a rooted planar map M endowed with two different α -orientations for the function α with $\alpha(v) = 2$ for every vertex v. The second orientation can be obtained from the first one by performing a flip on the counterclockwise cycle highlighted in red. Note that both orientations are accessible and that the second orientation is minimal, since it does not contain a counterclockwise cycle anymore.





(a) An orientation containing a ccw cycle.

(b) A minimal orientation.

Figure 3.7: Performing a flip from the left to the right orientation.

Since the in-degrees of the involved vertices are not changed after performing such a flip, a given α -orientation is still an α -orientation after performing any sequence of flips. Moreover, the accessibility of an orientation is preserved under flips. In [Fel04] it is shown that we can commute between any two α -orientations this way, leading to the following result.

Theorem 3.1.15: (Felsner [Fel04]) Let M be a planar map with a root face and α be a feasible function on its vertices. Then, there exists a unique minimal α -orientation.

For any given feasible α -orientation, we can thus use this theorem to canonically associate one specific minimal α -orientation.

³Note that in [AP15] the definition is stated in the opposite direction; here we follow the convention that is also used in other sources.

We continue with some definitions regarding blossoming maps in addition to those introduced in the previous subsections.

Definition 3.1.16: Let M be a blossoming map endowed with an orientation. The local closure is defined analogously to the closure operation introduced earlier. The newly created closure edge is oriented from the (former) opening stem to the (former) closing

The **interior** M° of a blossoming map M is the non-blossoming object obtained from M by removing all its stems.

The **interior degree** of a vertex v is the degree of v in M° .

The **degree** of a vertex v in a blossoming map is the sum of its interior degree and the number of stems adjacent to it.

In the first subfigure of Figure 3.8, a vertex-rooted blossoming tree endowed with an accessible and minimal orientation is illustrated. The second subfigure depicts the blossoming map after a single local closure, and the final subfigure shows the result after all possible local closures have been performed. Since the original map had an equal number of opening and closing stems, the complete closure yields a non-blossoming map.

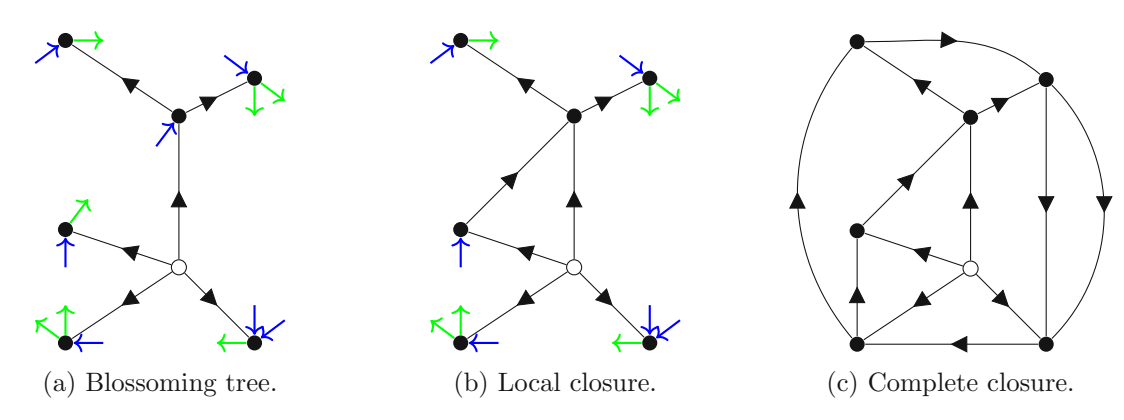


Figure 3.8: The steps of the complete closure applied to a vertex-rooted blossoming tree.

In this example, the resulting map also inherits an accessible and minimal orientation. The following lemma gives a sufficient condition for creating such an orientation.

Lemma 3.1.17: Let T be a blossoming tree endowed with an accessible orientation. The complete closure \overline{T} is then endowed with an accessible and minimal orientation.

Proof. Adding new edges cannot destroy accessibility, since all original directed paths remain present in T. The orientation of T is minimal because a tree does not contain any (counterclockwise) cycle. Each newly added closure edge is inserted from an opening to a closing stem in clockwise order, which places the outer face on its left. This means that any local closure cannot introduce a counterclockwise cycle and preserves the minimality of an orientation.

When considering a vertex-rooted blossoming tree T, the only way to endow it with an accessible (and minimal) orientation is to orient each edge away from the root vertex. As stated in Lemma 3.1.17, the closure \overline{T} of the oriented tree is then also endowed with an accessible and minimal orientation. If, in addition, T has an equal number of opening and closing stems, its closure is a non-blossoming vertex-rooted map.

We now present the **opening** which recovers the original blossoming tree T from its complete closure \overline{T} .

For a vertex-rooted plane map M, we define an **opening edge** as an edge that has the outer face on its left and whose deletion does not destroy accessibility. To apply the algorithm, select any opening edge and replace its two half-edges with the corresponding opening and closing stems

Algorithm 3 Opening algorithm for maps endowed with a minimal and accessible orien-

Require: M vertex-rooted plane map endowed with a minimal and accessible orientation, c the cyclic contour word of M

```
1: e_0 \leftarrow a random outer edge
2: while M is not a tree do
        e_1 \leftarrow e_0
        e_0 \leftarrow the edge after e_1 in c
4:
        if e_1 is an opening edge then
5:
 6:
            f \leftarrow the (inner) face on the right of e_1
            m \leftarrow \deg(f)
 7:
            update c by substituting the letter e corresponding to e_1 by \bar{b}e^{m-1}\bar{b}
 8:
            update the map M accordingly
9:
        end if
10:
11: end while
12: return vertex-rooted blossoming tree M
```

The proof in Section 4.2 shows that Algorithm 3 always terminates, since an opening edge can be found whenever M is not a tree. It also establishes that the resulting blossoming tree is uniquely determined. It follows that the opening algorithm is precisely the inverse of the closure operation, hence we can state the main theorem for our bijective approach.

Theorem 3.1.18: Let M be a vertex-rooted plane map endowed with an accessible and minimal orientation O. The opening algorithm yields the unique vertex-rooted blossoming tree with its accessible orientation, whose closure is M oriented with O.

For certain families of plane maps, the previous theorem implies a bijection with a corresponding family of blossoming trees via the opening algorithm.

Corollary 3.1.19: If \mathcal{M} is a family of plane maps with each map canonically endowed with an accessible and minimal orientation, there exists a bijection between \mathcal{M} and a family of blossoming trees with the same distribution of in- and out-degrees.

We illustrate this strategy by recovering Schaeffer's bijection for planar Eulerian maps with prescribed vertex degrees, as introduced in Subsection 3.1.1. It is well-known that Eulerian maps can equivalently be defined as follows.

Definition 3.1.20: A map is called **Eulerian** if there exists an **Eulerian cycle**⁴ that traverses every edge of the map exactly once.

From this definition, an Eulerian map M naturally admits an Eulerian orientation in which every vertex v satisfies $\deg_M^-(v) = \deg_M^+(v)$. This orientation is derived from the directed Eulerian cycle; thus the Eulerian orientation is accessible. An accessible and minimal Eulerian orientation can be obtained recursively: first, orient the outer edges of the map clockwise and remove the edges belonging to this clockwise cycle. Since the degree of each vertex incident to the cycle is reduced by 2, the connected components (possibly more than one) are Eulerian maps. Repeating this procedure until no edges remain yields an Eulerian orientation that contains no counterclockwise cycle.

Theorem 3.1.21: Let M be a planar rooted Eulerian map with d_i vertices of degree 2ifor $i \in \mathbb{N}$, endowed with its minimal Eulerian orientation. Applying the opening algorithm to M yields a rooted blossoming tree T in which every vertex corresponding to a vertex of degree 2i in M satisfies $deg_T^-(v) = deg_T^+(v) = i$.

Proof. Each vertex of degree 2i in M has in- and out-degree i in the map endowed with an Eulerian orientation. The opening algorithm replaces each of the two half-edges of a directed edge by their corresponding opening and closing stem without changing the vertex degrees, so the property is preserved in T.

This does not immediately recover the bijection from Subsection 3.1.1, as a slight modification of the opening algorithm is required. In this case, we choose the root edge of the Eulerian map as the first step in the algorithm; being an outer edge, it has the outer face on its left and can be deleted without destroying accessibility. Substitute its two half-edges by the corresponding opening/closing stem as usual, but then replace the closing stem by another opening stem, and mark it. In this way, you get a balanced Eulerian blossoming tree as in Subsection 3.1.1 instead of a rooted blossoming tree as in the previous theorem.

The enumeration of rooted blossoming trees with the prescribed vertex-degree distribution – and hence of planar rooted Eulerian maps – can be carried out analogously to the method described in Subsection 3.1.1.

3.1.4 p-gonal d-angulations

We now apply the general bijective scheme of the previous subsection to establish a bijection between p-gonal d-angulations of girth d and p-gonal d-fractional forests, as described in Section 5 of [AP15].

This construction generalizes the bijection obtained for simple triangulations in Subsection 3.1.2.

Unlike in other sources, we do not use the canonical plane embedding of face-rooted maps with the root face as the outer face. Instead, we consider only face-rooted plane maps in which the outer face and the root face are different. Although this choice yields equivalent enumerative results, it provides technical advantages in the bijective construction, as discussed in [AP15].

⁴We slightly deviate from our previous notation of a cycle and allow for revisiting vertices.

Definition 3.1.22: The **girth** of a map is the length of its shortest cycle.

For a given $d \in \mathbb{N}$, any d-angulation has girth at most d (unless it is a tree). In this subsection, we will restrict ourselves to d-angulations having girth exactly d. We even generalize the notion of a d-angulation for our purposes.

Definition 3.1.23: For $3 \le d \le p$, a *p*-gonal *d*-angulation is a plane map of girth *d*, in which a face different from the outer face is additionally marked. The boundary of the marked face is a cycle of length p, each other face has degree d.

We call a vertex **marked** if it belongs to the boundary of the marked face.

Definition 3.1.24: For $k \in \mathbb{N}$, a k-partial direction of an edge e is a choice of direction for k copies of e, where the order of the edges does not matter. A partial direction of an edge is usually depicted as a certain number of arrows going in each of the two directions. A k-fractional orientation of a plane map is the choice of a k-partial direction for each edge of the map. In this setting, an edge is called **saturated** if all its copies are oriented in the same direction.

In this setting, an edge is called **saturated** if all its copies are directed in the same direction.

Given a plane map M, the k-expanded version of M is obtained by replacing each edge with k copies. The previous definition of a k-fractional orientation can then be interpreted as an orientation of the k-expanded map, in which two copies of an edge are not allowed to create a counterclockwise cycle.

Using this interpretation for a map endowed with a k-fractional orientation, the inand out-degree of a vertex v, as well as notions such as clockwise and counterclockwise cycles, minimality, and accessibility, are defined with respect to the orientation of the corresponding k-expanded map.

Definition 3.1.25: For any $j,k \in \mathbb{N}$, a j/k-orientation of a plane map with a marked face is defined as a k-fractional orientation such that $\deg^-(v) = k$ for each marked vertex and $\deg^-(v) = j$ for every other vertex, and the boundary of the marked face is a directed clockwise cycle of saturated edges.

Figure 3.9 illustrates a 5-angulation of girth 5 endowed with a 5/3-orientation. We will later show that d/(d-2)-orientations play a central role for d-angulations. This consideration raises the question of whether we can also endow a p-gonal d-angulation with a d/(d-2)-orientation whenever $p \neq d$.

Lemma 3.1.26: Let M be a p-qual d-angulation endowed with a (d-2)-fractional orientation, such that $deg^-(v) = d$ for every non-marked vertex v. The sum of in-degrees of the marked vertices is equal to (d-2)p + (p-d).

Proof. For any p-gonal d-angulation, we have 1 face of degree p and |F(M)|-1 faces of degree d. Applying Formula 2.1 gives $p+d(|F(M)|-1)=2\cdot |E(M)|$. Using Euler's formula, we can eliminate |F(M)| and rearrange to

$$(d-2)|E(M)| = d \cdot |V(M)| - p - d$$

$$= d(|V(M)| - p) + dp - p - d$$

= $d(|V(M)| - p) + (d - 2)p + (d - p).$

Since d(|V(M)| - p) is the sum of in-degrees of the non-marked vertices, the remaining term must be the sum of in-degrees of the marked vertices.

The consequence of this lemma is the following. If we require the degree condition for all non-marked vertices of a map M, then among the p marked vertices, there must be at least one vertex v with $deg^-(v) > d-2$. Consequently, when p > d, it is impossible to find a (d-2)/d-orientation. This justifies the following definition.

Definition 3.1.27: For any $j, k \geq 0$, a **pseudo-**j/k**-orientation** of a plane map with a marked face is defined as a k-fractional orientation such that $\deg^-(v) = j$ for every non-marked vertex, and the boundary of the marked face is a directed clockwise cycle of saturated edges.

Figure 3.9 shows a 5-angulation of girth 5 with its minimal 5/3-orientation, and a 4-gonal triangulation of girth 3 with its minimal pseudo-3/1-orientation.

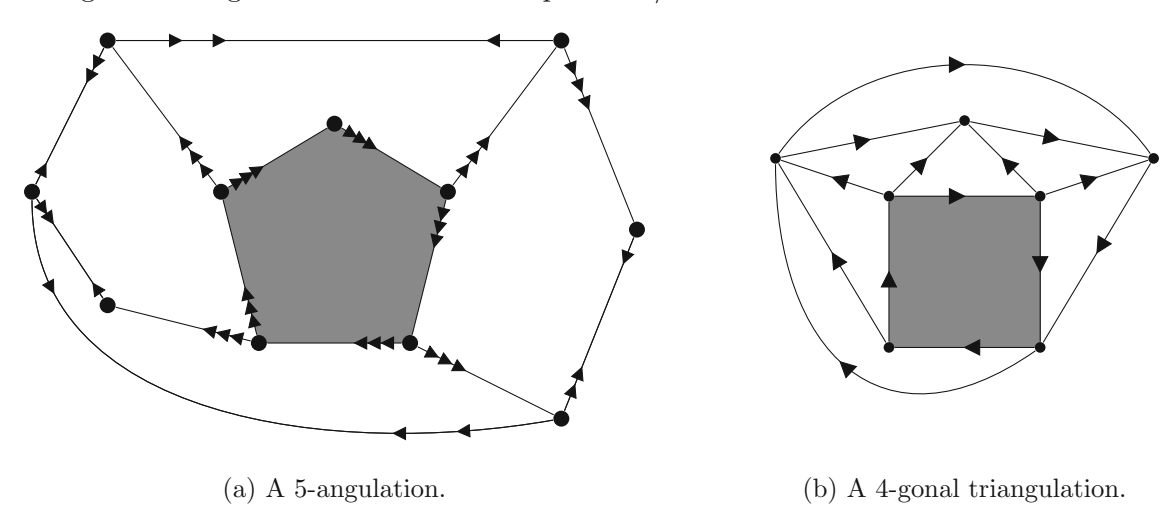


Figure 3.9: Two d-angulations endowed with a (pseudo-)d/(d-2)-orientation.

In fact, for any $d \geq 3$ the property of a (p-gonal) d-angulation having girth d can be characterized by the existence of a (pseudo-)d/(d-2)-orientation.

Theorem 3.1.28 ([BF11], Theorem 13 and Proposition 19): Let $d \geq 3$ and M be a dangulation with a marked face. M admits a d/(d-2)-orientation if and only if it has girth d.

Let $p \ge d \ge 3$ and M be a p-gonal d-angulation. M admits a pseudo-d/(d-2)-orientation if and only if it has girth d.

In both cases, these orientations are accessible and there exists a unique minimal (pseudod/(d-2)-orientation among them.

To apply the results of Subsection 3.1.3, we need to introduce a new family of planar maps.

Definition 3.1.29: A p-cyclic forest is a plane map with exactly two faces: the outer face and a marked face, whose boundary is a simple cycle of length p. A p-cyclic forest can be seen as a cycle of p planted plane trees.

For $d \geq 3$ and $0 \leq i \leq d-2$, a d-fractional tree of excess i is a planted blossoming tree without opening stems endowed with an accessible (d-2)-fractional orientation such that $\deg^-(v) = i$ for the root vertex and $\deg^-(v) = d$ for each non-root vertex. In this setting, a closing stem attached to a vertex v is counted as contributing d-2 to the in-degree of v. For $p \ge d \ge 3$, a p-gonal d-fractional forest is a p-cyclic forest, whose planted trees are d-fractional trees. The excesses of those trees are required to sum up to p-d.

In Figure 3.10a, a 5-gonal 5-fractional forest is illustrated. Only one of its planted trees is a non-trivial 5-fractional tree; the other four planted trees in the cycle each consist of a single vertex. Figure 3.10b shows a 4-gonal 3-fractional forest. The sum of excesses is 4-3=1 since only one of the four 3-fractional trees has an excess 1 greater than zero.

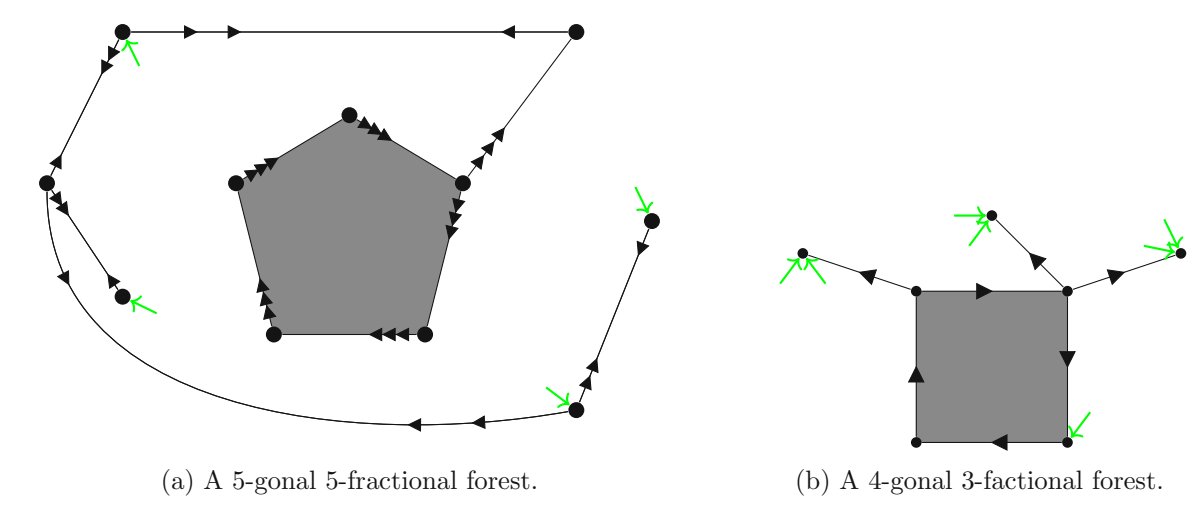


Figure 3.10: Two d-fractional forests endowed with a (pseudo-)d/(d-2)-orientation.

The maps in Figure 3.10 closely resemble those in Figure 3.9, and we now outline how they are connected. For any p-gonal d-angulation of girth d endowed with its minimal (pseudo)d/(d-2)-orientation, we can contract the marked face into a single vertex, obtaining a vertex-rooted plane map endowed with a minimal accessible (d-2-fractional) orientation. After this step, we can use a variant of the opening Algorithm 3. In the previous subsection, we only introduced "normal" orientations, but all the algorithms and theorems are also valid for k-fractional orientations since we can reduce those to orientations of the corresponding k-fractional maps.

Given a vertex-rooted plane map M endowed with a k-fractional orientation, we define an opening edge as a saturated edge that has the outer face on its left (i.e., each of its corresponding copies has) and whose deletion does not destroy accessibility. We again perform an exhaustive deletion of opening edges, but in each step we substitute the edge only by a closing stem and omit the corresponding opening stem. We do this in order to simplify the enumeration of these forests. This is an analog to showing only the opening stems in the case of triangular blossoming trees. In the case of d-fractional forests, the local

closure is not a substitution of a factor bee by the letter e but a substitution of a factor $e^{d-1}\bar{b}$ by the letter e in the corresponding contour word.

This variant of the opening algorithm suggests an application of the master bijection. Theorem 3.1.18 implies that the opening produces a p-gonal d-fractional forest. Since we omit the opening stems during the variant of the opening algorithm, we need to check that the corresponding variant of the closure of a p-gonal d-fractional forest indeed produces a p-gonal d-angulation. The inner faces are of degree d by construction, the degree of the outer face needs to be verified. See the proof of Theorem 5.6 in [AP15].

These considerations yield the following main theorem of this section.

Theorem 3.1.30: There exists a bijection between p-gonal d-fractional forests with n vertices and p-gonal d-angulations of girth d with n vertices.

An interesting consequence of this bijective result is that we can now enumerate dangulations of girth d simply by counting d-fractional forests. The latter can be enumerated more easily due to their structure as cycles of d-fractional trees. In [AP15], a formula for the generating function $M_{d,p}(x)$ of corner-rooted p-gonal d-angulations of girth d with a marked outer face and counted according to the number of non-root faces is given. For any $j \in \mathbb{N}^+$, let h_j be the polynomial in the variables t_1, t_2, \ldots defined by

$$h_j(t_1, t_2, \dots) := [x^j] \frac{1}{1 - \sum_{i>0} x^i t_i} = \sum_{r>0} \sum_{\substack{i_1, \dots, i_r > 0 \\ i_1 + \dots + i_r = j}} t_{i_i} \cdots t_{i_r}$$

and T_i by

$$T_i(x) = \frac{1}{1 - T_0} \cdot h_{i+2} \left(\frac{T_1}{1 - T_0}, \dots, \frac{T_{d-3}}{1 - T_0}, \frac{x}{1 - T_0} \right),$$

for $0 \le i \le d-3$ and $T_i = 0$ otherwise.

The generating function is then given by

$$M_{d,p}(x) = x \left(\frac{1}{1-T_0}\right)^p \cdot h_{p-d}^{(p)} \left(\frac{T_1}{1-T_0}, \dots, \frac{T_{d-3}}{1-T_0}, \frac{x}{1-T_0}\right).$$

3.1.5 Generalization to maps of higher genus

Even though the focus of this thesis is on planar maps, it is interesting to present a little introduction to maps of higher genus and to how the previously presented concepts have been generalized. We will present the generalizations of the CVS bijection to maps on an orientable and non-orientable surface of any genus and follow the ideas of [CD17] and [DL22].

Definition 3.1.31: A surface S is a compact, connected, two-dimensional real manifold. Surfaces are considered up to homeomorphism.

For any surface S, we can obtain a new surface S' by adding so-called **handles** or cross-caps. We refer to Chapter 3 of [MT01] for a thorough introduction to the topic of surfaces.

Definition 3.1.32: For any $g \in \mathbb{N}$, we denote by \mathbb{S}_g the **torus** of **genus** g, that is, the orientable surface obtained by adding g holes to \mathbb{S}^2 . For any $g \in \frac{1}{2}\mathbb{N} \setminus \{0\}$, we denote by \mathcal{N}_g the non-orientable surface obtained by adding 2g cross-caps to \mathbb{S}^2 . In both cases, g is called the **type** of the surface.

Example 3.1.33: \mathbb{S}_0 is the sphere, \mathbb{S}_1 the torus, $\mathcal{N}_{1/2}$ the projective plane, and \mathcal{N}_1 the Klein

We now state the main theorem about the classification of surfaces.

Theorem 3.1.34 ([Tho92], Theorem 5.1): Let \mathbb{S} be a surface. Then \mathbb{S} is homeomorphic to precisely one of the surfaces \mathbb{S}_g for $g \in \mathbb{N}$ or \mathcal{N}_g for $g \in \frac{1}{2}\mathbb{N} \setminus \{0\}$.

These considerations enable us to define maps on general surfaces which generalizes our definition for planar maps.

Definition 3.1.35: A map of genus q is a proper embedding of a graph on a surface of genus q such that all its faces (connected components of the complement) are simply connected. We call a map (non-)orientable if its underlying surface is (non-)orientable.

Note that in the planar case, any unicellular map is a tree, which is not true on positivegenus surfaces.

Another fundamental result in the theory of maps on surfaces is the Euler characteristic formula which generalizes Euler's formula for planar maps.

Theorem 3.1.36: Let M be a map of genus g. Then

$$|V(M)| - |E(M)| + |F(M)| = 2 - 2g,$$

where $\chi := 2 - 2g$ is the **Euler characteristic** of the map.

In [Lep19], Schaeffer's construction for Eulerian maps is generalized to higher-genus orientable maps that are in one-to-one correspondence to a specific family of unicellular blossoming maps.

It is interesting to mention that the opening of [Sch97] was generalized by Bernardi in [Ber06]; this was then generalized for the higher-genus case by Bernardi and Chapuy in [BC11]. We now focus on a direct generalization of [Sch97].

In order to present the main theorem of the work, we first need to introduce some definitions.

Definition 3.1.37: A unicellular blossoming map is a map with only one face, in which each corner can carry a sequence of opening or closing stems. The number of opening and closing stems must be equal, and we require one of the opening stems to be marked.

The cyclic contour word is defined almost equally as in Definition 3.1.16. In this case, we omit the literal e and consider only the word on $\{b, b\}$.

Definition 3.1.38: An oriented unicellular map is called **well-oriented** if in a tour of the face starting from the marked opening stem, each edge is first traversed in the backward direction (against its orientation) and later in the forward direction (following its orientation).

Note that the definition does not depend on whether the tour is clockwise or counterclockwise. The well-orientation of a given unicellular map can be obtained by making a tour starting from the marked stem and orienting the edges backward whenever they are encountered first.

Definition 3.1.39: A well-oriented unicellular blossoming map is called **well-labeled** if it admits the labeling of the corners in the following way. We start at the corner that has the marked opening stem on its right and make a tour following this orientation.⁵ The first corner is labeled 0 and each following corner is increased/decreased by one if the corner is preceded by an opening/closing stem. If the corner is preceded by an edge, the label of the corner is chosen to be equal to the previous one. Whenever two corners are separated by an edge, we additionally require the label of the corner on the right side of the edge to be bigger by one.

A unicellular blossoming map is called **well-blossoming** if it is well-oriented and welllabeled.

Since a unicellular blossoming map must have the same number of opening and closing stems, the labeling process returns to the initial value 0 at the root corner after completing the tour.

Definition 3.1.40: A **Dyck word** on two literals (and) is a word on {(,)}, such that the number of (is equal to the number of) and each prefix of the word contains no more) than (.

Any word over an alphabet of two symbols can be interpreted as a one-dimensional walk, with a step up for the first symbol and a step down for the second. In this interpretation, Dyck words correspond precisely to walks that start and end at 0 and never go below 0.

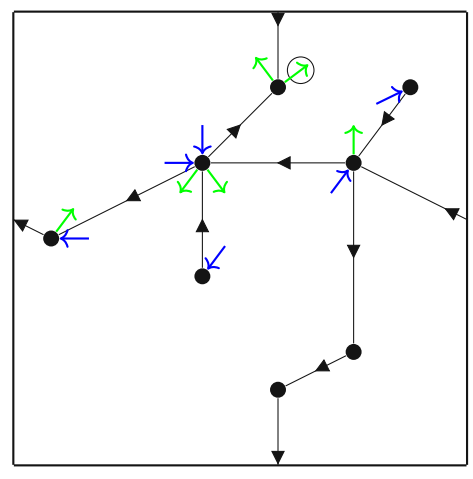
Definition 3.1.41: A unicellular blossoming map is called **well-rooted** if its contour word (starting at the marked opening stem) is a Dyck word on b and b.

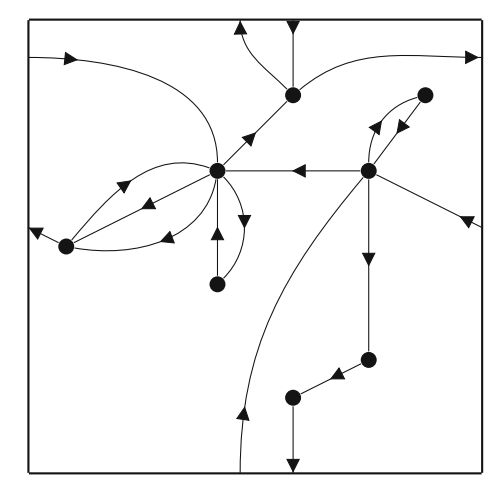
Under the interpretation of Dyck words as one-dimensional walks that never go below 0, a labeled unicellular blossoming map has all corner labels non-negative if and only if it is well-rooted. Thus, we could use this as an alternative definition.

In Figure 3.11a, we show a plane embedding of a well-rooted, well-blossoming unicellular blossoming map of genus 1 on the torus. The map is illustrated inside a square, with the left border identified with the right border and the top border identified with the bottom border. On the right side of the figure, we see a (non-blossoming) map with the same structure of vertices and the same distribution of vertex-degrees as the map on the left side. It can also be seen easily that the map on the right is bicolorable.

The example given in the figure exhibits a property known from Eulerian maps, namely that $\deg^-(v) = \deg^+(v)$ for every node v. This is in fact a general property of well-labeled, well-oriented unicellular blossoming maps, since the labels of corners around a vertex form a cycle of numbers differing by 1, with the higher label always to the right of the separating stem/edge.

⁵Although for non-orientable maps we lack the notion of clockwise and counterclockwise, a tour can still be defined analogously to Definition 2.2.5 for unicellular for maps on non-orientable surfaces.





(a) Unicellular map on the torus.

(b) Bicolorable map on the torus.

Figure 3.11: A unicellular blossoming map and its closure.

The map in Figure 3.11b is the generalized closure of the unicellular blossoming map similar to the closure of the previous subsections. In [Lep19], a generalized opening algorithm is also presented and proven to be the inverse of the generalized closure. Hence, the bijection of Schaeffer between planar Eulerian blossoming trees and planar Eulerian maps is generalized to maps of higher genus using conceptually similar algorithms of closure and opening.

Theorem 3.1.42 ([Lep19], Theorem 1.2): There exists a constructive weight-preserving and genus-preserving bijection between rooted bicolorable maps and well-rooted, well-blossoming unicellular blossoming maps.

We now outline how this result generalizes the bijection from Subsection 3.1.1 for planar maps. Recall from Lemma 2.1.27 that in the planar case there is an equivalence of bicolorable and Eulerian maps.

Eulerian blossoming trees can be interpreted as well-rooted, well-blossoming unicellular blossoming maps. A unique well-orientation is obtained by orienting each edge towards the marked stem, while the well-rooted condition is equivalent to our notion of "balanced" for Eulerian blossoming trees. Finally, the requirement that a vertex of degree 2i has i-1opening stems in an Eulerian blossoming tree guarantees that the corresponding unicellular blossoming map is well-rooted.

Using this theorem, the authors of [Lep19] also give a bijective explanation of an enumerative result obtained in 1991.

Theorem 3.1.43: [BC91] For any $g \ge 0$, the generating series $M_g(z)$ of orientable maps of genus g enumerated by edges is a rational function of z and $\sqrt{1-12z}$.

We emphasize that the previous considerations have dealt only with maps on orientable surfaces. In [DL22] the results are generalized to maps on any surfaces, orientable and non-orientable, and we now give a brief overview of the results obtained there.

The definitions of the considered objects remain almost unchanged; the only modification is the introduction of a notion of color for stems and faces.

Definition 3.1.44: An opening or closing stem is called **black/white** if the minimum of the labels of all adjacent corners is odd/even. On the other hand, a face is called black/white if the minimum of the labels of all adjacent corners is even/odd.

The main result of [DL22] is the following bijection.

Theorem 3.1.45: Let \mathbb{S} be a surface, and $n_{\bullet}, n_{\circ}, n_{1}, n_{2}, \ldots$ be integers with finite sum. There exists a bijection Φ between bipartite pointed maps of $\mathbb S$ with

- n• black vertices.
- n_{\circ} white vertices,
- n_k faces of degree 2k (for any $k \in \mathbb{N}^+$);

and well-blossoming unicellular blossoming maps of S with

- the total number of black leaves and black faces equal to n_{\bullet} ,
- the total number of white leaves and white faces equal to n_{\circ} ,
- n_k vertices of degree 2k (for any $k \in \mathbb{N}^+$).

Moreover, the image $\Phi(M)$ is well-rooted if and only if M is a root-pointed map.

This result not only extends the work of [Lep19] by including non-orientable surfaces, but it further enables the study of metric properties through the bijection, since it deals with pointed maps. We also mention that this bijection deals with bipartite maps, while the bijection in the orientable case deals with bicolorable maps. Recall that bipartiteness and bicolorability are dual concepts, which suggests a natural connection between the two settings. The difference comes from the fact that the closure and opening algorithms are defined differently in [DL22]. In the closure algorithm, first a bicolorable map (with a marked face) is obtained, and then the dual of this map is taken in order to obtain the bipartite pointed map. In [DL22], the closure algorithm first constructs a bicolorable map with a marked face and then takes its dual to obtain the bipartite pointed map. The construction proceeds by working with both the original map and its dual in order to obtain the unicellular blossoming map.

3.2 Bijections of category (B)

We now turn to bijections between a class of maps and a class of decorated trees. In general, the decorated tree is no longer a spanning tree of the corresponding map. In many cases the decorated tree has vertices of two colors. We will call those bijections of category (B).

3.2.1 The CVS Bijection

The Cori-Vauquelin-Schaeffer (CVS) bijection [CV81; Sch98] establishes a fundamental correspondence between planar rooted quadrangulations and well-labeled trees, serving as a basis for enumerative and metric studies of planar maps, and for further research in this field.

In this subsection, we will mainly use the notation of [CD17]. The paper is designed to prove the CVS bijection for the general case of maps on any surface, but we will limit ourselves to the case of planar maps for now. A further discussion of the general case is postponed to Subsection 3.2.6.

Definition 3.2.1: Let M be a map with a root vertex v_0 . The **geodesic distance** of a vertex v is defined as its distance $d(v, v_0)$ to the root vertex.

We show a result that will be essential for our further considerations.

Lemma 3.2.2: Let M be a bipartite map with a root vertex and every vertex labeled by its geodesic distance. The labels of two adjacent vertices differ by exactly 1.

Proof. The labels of two adjacent vertices cannot differ by more than 1. Let v_1 and v_2 be two adjacent vertices connected by an edge e and assume that their labels are both equal to $k \in \mathbb{N}^+$. By definition, there exists a shortest path p_i from v to v_i of length k (for i = 1, 2). There exists a single vertex w that lies on both paths and has the property that the paths \tilde{p}_i from w to v_i are disjunct paths of length j with $1 \leq j \leq k$. The path $\tilde{p}_1 e \tilde{p}_2$ is now a cycle of odd length 2j+1, which contradicts the bipartiteness of the map.

According to Lemma 2.1.22, planar quadrangulations are bipartite. Thus, due to the previous lemma, for any face of a quadrangulation, the labels of the vertices on the (clockwise) border yield a (cyclic) sequence of the form (i-1,i,i-1,i) or of the form (i-1,i,i+1,i)for some $i \geq 1$. This motivates the following definition.

Definition 3.2.3: In a quadrangulation, a face is called **simple/confluent** if the labels of the vertices on its border yield a (cyclic) sequence of the form (i-1,i,i-1,i) / (i-1,i,i-1,i)1, i, i+1, i). For each face of a quadrangulation we call **local operation** the process of adding a new edge connecting the two corners where the vertex label increases relative to the preceding corner in clockwise order.

The local operations for a simple and a confluent face are illustrated in Figure 3.12; the newly created edges are depicted in red. The newly added oriented edges can be ignored for now.

Definition 3.2.4: Let M be a quadrangulation with a root vertex v_0 . By $\Phi(M)$ we denote the graph defined by performing the local operation on each face of M, then deleting v_0 and all edges of the original map M. The map Φ is rooted by adding a root corner instead of the former root edge.

Figure 3.13 illustrates the transformation of a quadrangulation M with 5 faces into $\Phi(M)$. On the right side of the figure, the superimposition of the original map M (dashed edges) and the map $\Phi(M)$ (red edges) is shown.

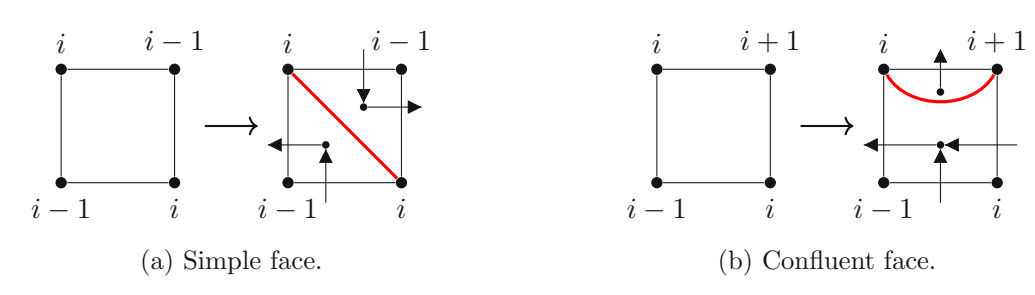


Figure 3.12: Local operations and DEG.

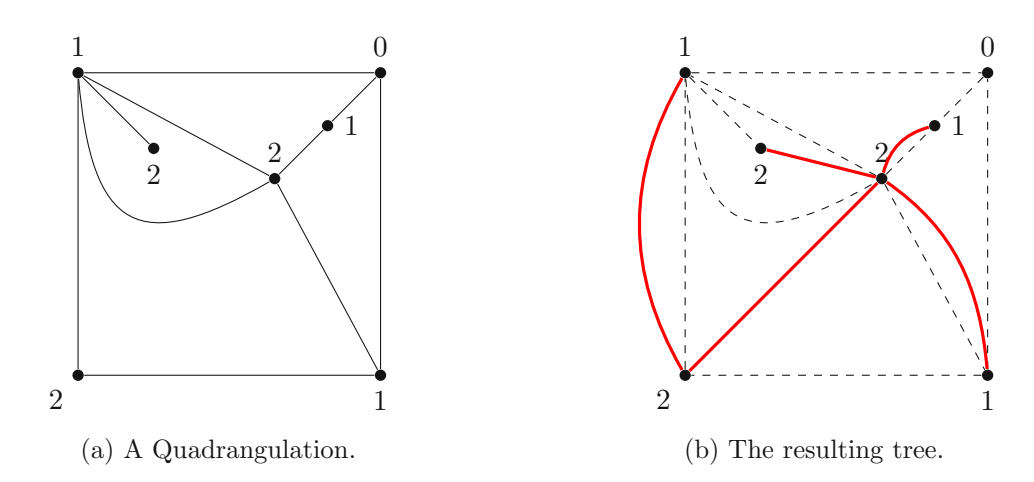


Figure 3.13: A rooted quadrangulation M and its corresponding well-labeled tree.

Definition 3.2.5: Let M be a quadrangulation with a root vertex endowed with its geodesic labeling. We define the dual exploration graph (DEG) as follows:

- 1. Place a vertex f^* inside each face f of the map $M \cup \Phi(M)$.
- 2. For each edge $e = \{v_1, v_2\}$ of M, where v_1, v_2 have labels i, i+1, respectively, add an edge across this edge connecting the vertices f_1^*, f_2^* corresponding to the two faces f_1, f_2 adjacent to e. Orient the edge so that the vertex v_2 with the higher label i+1is on its right.

Although for our current purposes, the DEG could be considered as an undirected map, we retain the original orientation conventions of [CD17] to facilitate further engagement with the topic.

Note that the DEG is not even necessary for defining the CVS bijection in the planar case. Still, we define it here in order to work with it in subsequent subsections.

We want to show that the map $\Phi(M)$ is a tree on the vertex set $V(M) \setminus \{v_0\}$. The idea is to prove this, using the following lemma about the structure of the DEG.

Lemma 3.2.6: The DEG of a quadrangulation with root vertex v_0 contains only one (directed) cycle. This cycle is around the vertex v_0 and can be contracted into a single vertex. Hence, the contracted DEG is a tree.

We will prove this lemma in Section 4.1 and use it here already to show the statement about the map $\Phi(M)$. We prove it by applying Theorem 2.1.26.

Note first that the (undirected) DEG is a subgraph of the dual of the map $M \cup \Phi(M)$. In fact, it consists of all edges dual to the edges in M (and therefore not in $\Phi(M)$).

Consider now the map M' obtained from the map $M \cup \Phi(M)$ by deleting the vertex v_0 and all its incident edges. The construction of M' corresponds to contracting the cycle around the vertex v_0 into a single vertex in the dual $(M \cup \Phi(M))^*$; this yields the dual map $(M')^*$. Now, by the previous lemma, the contracted DEG is a spanning tree of $(M')^*$. As mentioned above, $\Phi(M)$ is the complement of the edges dual to the DEG. By Theorem 2.1.26, $\Phi(M)$ is a spanning tree of the map M', which has the vertex set $V(M) \setminus \{v_0\}$.

Theorem 3.2.7: For a quadrangulation M with root vertex v_0 , the map $\Phi(M)$ is a welllabeled tree on the vertex set $V(M) \setminus \{v_0\}$.

Since each face of M corresponds to one edge in $\Phi(M)$, the mapping Φ sends planar rooted quadrangulations with n faces to well-labeled rooted plane trees with n edges.

In order to give the inverse construction of the mapping Φ , we introduce a function on the corners of a map.

Definition 3.2.8: Let M be a map with root vertex v_0 and let F be a face of degree k incident to v_0 . Label each vertex and, thus, also each corner with its geodesic distance. Enumerate the corners of F from 0 to k-1 in clockwise order, starting at the corner incident to v_0 . The label of each corner $0 \le i \le k-1$ is then denoted by l_i . The successor function s is defined as

$$s(i) = \inf\{j > i : l_j = l_i - 1\}$$

for any corner i.

The successor function plays a crucial role in Algorithm 4, which is proved to be the reverse construction, and is called the closing of a well-labeled rooted plane tree.

We denote by T_0 the map obtained after the first for-loop. If j is the number of corners in T incident to a vertex with label 1, the map T_0 has j faces. Note that each of these faces satisfies the conditions of Definition 3.2.8, allowing us to use the successor function in the remainder of the algorithm.

We prove the correctness of this algorithm in Section 4.1 and establish the following bijective theorem.

Theorem 3.2.9: The mapping Φ is a bijection between the set of planar rooted quadrangulations with n faces and the set of well-labeled rooted plane trees with n edges. The mapping has the following property: Let Q be a quadrangulation with root vertex v_0 and $T := \Phi(Q)$ the associated tree. For every vertex $v \in V(Q) \setminus \{v_0\}$, we have

$$d_Q(v, v_0) = l_v, (3.3)$$

i.e., the geodesic distance in Q is equal to the label in T.

Algorithm 4 Closing of a well-labeled rooted plane tree Ψ

```
Require: T a well-labeled plane tree
 1: add a vertex v_0 with label 0
 2: for c corner incident to a vertex with label 1 do
        add an edge e from v_0 to c
        if c is the root corner of T then
 4:
           let e be the new root edge
 5:
        end if
 6:
 7: end for
 8: for f face of T_0 do
        for i corner of f do
 9:
10:
           if s(i) \neq i+1 then
               add an edge \{i, s(i)\}
                                                                          \triangleright also called a chord
11:
           end if
12:
        end for
13:
14: end for
15: delete all edges whose endpoints have equal label
16: return \Psi(T)
```

From Property (3.3), we can derive an upper bound for the distance between two vertices $v_1, v_2 \in V(Q) \setminus \{v_0\}$ which is useful for our geometric analysis in Section 5.2. We get

$$d_Q(v_1, v_2) \le l_{v_1} + l_{v_2} - 2 \max\left(\min_{w \in [v_1, v_2]} l_w, \min_{w \in [v_2, v_1]} l_w\right),\tag{3.4}$$

where the interval notation $[v_1, v_2]$ denotes the set of all vertices visited on the clockwise tour around the tree from v_1 to v_2 .

The CVS bijection can be modified to obtain a new mapping $\tilde{\Phi}$. This variant of the bijection turns out to be a bijection as well.

Theorem 3.2.10: The mapping Φ is a bijection from the set of planar pointed quadrangulations with n faces and a disjoint union of two copies of the set of labeled rooted plane trees with n edges.

The factor of two corresponds to the choice of the root edge orientation of the pointed quadrangulation.

3.2.2 The BDG Bijection

The bijection of Bouttier, Di Francesco, and Guitter [BFG04] describes the general case of Eulerian planar maps with prescribed face degrees and introduces a new class of labeled trees. The term mobile will be used throughout this section and appears here for the first time. The BDG bijection also applies to quadrangulations and, consequently, covers the CVS bijection.

In Section 2 of the paper, the focus is on planar maps whose faces all have even degrees and are thus bipartite. In Section 3 the construction is extended to the more general class of Eulerian (face-bicolored) maps with prescribed numbers of faces of given colors and degrees.

Recall that for a bipartite map endowed with the geodesic distance labeling, the labels of the contour of a face form a cyclic sequence with increments ± 1 . As shown in Lemma 2.1.22, in the planar case, every even map is bipartite, and the above observation therefore applies to even maps as well. For a face f of degree 2k, exactly half of the corners are, in clockwise order, followed by a corner of smaller label. We denote the set of these k corners by S_f .

With this notion, we describe Algorithm 5 that transforms a vertex-rooted even planar map M, endowed with its geodesic labeling, into a bicolored tree.

Algorithm 5 BDG construction for vertex-rooted even planar maps

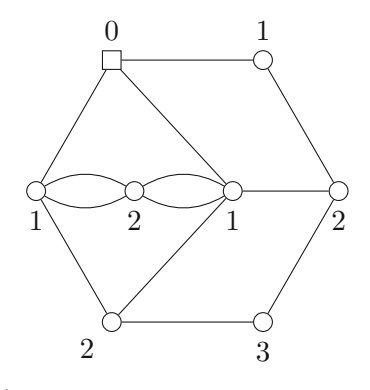
```
Require: M a vertex-rooted even planar map
```

```
1: for f face of M do
```

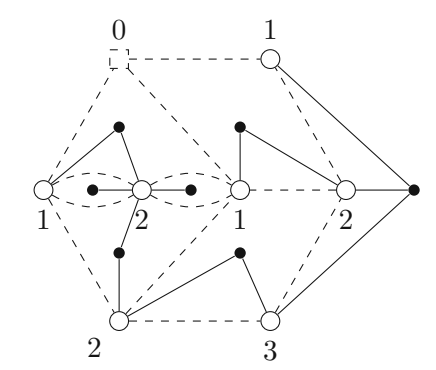
- $2k \leftarrow \deg(f)$
- add a new black vertex f^* inside f3:
- for $c \in S_f$ do 4:
- $\triangleright |S_f| = k$ add an edge from f^* to the white vertex incident to c5:
- end for 6:
- 7: end for
- 8: delete all edges of the original map
- 9: delete the root vertex v_0

- \triangleright By construction, v_0 has no incident edge
- 10: **return** the resulting map

In Figure 3.14, the vertices of the original map are depicted in white.



(a) Vertex-rooted even planar map.



(b) The resulting tree.

Figure 3.14: An even map and its corresponding well-labeled Eulerian mobile.

The resulting structure is a plane tree with vertices of two colors which forms an instance of a general class of decorated trees.

Definition 3.2.11: We define an **Eulerian mobile** as a plane tree with vertices colored



either black or white, such that every edge connects a black vertex to a white vertex. An Eulerian mobile is called **labeled** if every white vertex carries an integer label and for each black vertex, the labels n and m of two consecutive white neighbors in clockwise order satisfy $m \ge n-1$. If all labels are positive and there is at least one vertex that has label 1, the Eulerian mobile is called **well-labeled**.

In Algorithm 6, we define a mapping on well-labeled Eulerian mobiles that reconstructs the original even planar map. We assume that all corners of the unique face of the mobile are enumerated starting from a corner that is preceded by a corner of label 1. For the use of the successor function from the previous subsection in the algorithm, it does not matter which corner of label 1 is chosen for this purpose.

Algorithm 6 BDG construction for well-labeled Eulerian mobiles

Require: T a well-labeled Eulerian mobile

- 1: for c white corner of T with label $n \geq 2$ do
- add an edge $\{c, s(c)\}$
- 3: end for
- 4: $F_0 \leftarrow$ the face that is incident to all vertices of label 1
- 5: add a white root vertex v_0 with label 0 in F_0
- 6: for c white corner with label 1 incident to F_0 do
- 7: add an edge between c and v_0
- 8: end for
- 9: delete all black vertices and their incident edges
- 10: **return** the resulting map

Remark 3.2.12: In the original paper, the face F_0 is called the outer face. Since we are actually not working with plane/face-rooted maps here, we decided to be more precise and define the face F_0 this way.

Whenever new edges are added to the mobile T, this is done in such a way that there are no intersecting edges. We refer to [BFG04] for the proof that the construction is welldefined and that it is indeed the inverse of the previous construction in Algorithm 5. We state the bijective theorem here.

Theorem 3.2.13: There exists a bijection between vertex-rooted even planar maps with n vertices and m faces and well-labeled Eulerian mobiles with n-1 white and m black vertices. Moreover, each face of degree 2k corresponds to a black vertex of degree k.

In Section 3 of [BFG04], the BDG construction is further generalized into a bijection between planar face-bicolored (and hence Eulerian) maps with fixed numbers of faces with prescribed color and degree and so called well-labeled generalized mobiles. Since the construction is very similar to the previous one, we will not go into it any further.

Theorem 3.2.14: There exists a bijection between planar face-bicolored vertex-rooted Eulerian maps with n vertices, m black faces, l white faces and well-labeled generalized mobiles with n-1 labeled vertices, m unlabeled black vertices, l unlabeled white vertices.

We show only how this construction covers the bipartite case. Given any bipartite map M, we can substitute each edge by a double edge, and hence create new (black) faces of degree two; each original face of M remains the same and is colored white. Thus, any bipartite map can be represented as a face-bicolored map with fixed numbers of faces with prescribed color and degree.

Using the same strategy of substituting each edge by a double edge, we can also generalize this bijection for arbitrary planar maps with prescribed face degrees. In particular, quadrangulations form a special case in which all faces have degree 4.

3.2.3 Unified bijective scheme

We present some kind of unified bijective scheme similar to the one in Subsection 3.1.3. Here it is called "master bijection" and relies on finding canonical orientations for certain classes of maps which generalizes previous bijections of this section. The master bijection here produces a spanning tree of the superimposition of a planar map, its dual and their common quadrangulation. We mainly follow the notations of [BF11; BF12].

Definition 3.2.15: A biorientation of a map is the choice of a direction for each halfedge. A half-edge is called **ingoing/outgoing** if it is oriented toward/from its incident vertex. For $i \in \{1,2,3\}$, we call an edge i-way if it has exactly i ingoing half-edges (see Figure 3.15). The **in-degree/out-degree** of a vertex is the number of its incident ingoing/outgoing half-edges. The **clockwise degree** of a face f is the number of outgoing half-edges incident to f having f on their right. In a biorientation, we define a **directed path** if there exist distinct vertices v_1, \ldots, v_k , such that for all $i = 1, \ldots, k-1$ the edge $\{v_i, v_{i+1}\}\$ is either 2-way or 1-way oriented toward v_{i+1} . A directed cycle is a directed path which is closed $(v_0 = v_k)$. A biorientation is called **accessible** from a vertex v if for every vertex w, there exists a directed path from v to w. In a map with a root face, a directed cycle is called **counterclockwise** if each of its edges has the outer face on its left. A map endowed with a biorientation is called **minimal** if it has no counterclockwise cycle.

We want to emphasize here that the notion of a biorientation generalizes the orientations previously introduced. An orientation is a biorientation that consists only of 1-way edges.

From now on, we will also use the term (planar) biorientation for the map itself that is endowed with the biorientation.

Definition 3.2.16: A weighted biorientation is obtained by associating a weight $w(h) \in \mathbb{R}$ to each half-edge h. The weight of an edge is the sum of the weights of its two half-edges. The weight of a face f is the sum of the weights of all outgoing half-edges incident to fhaving f on their right.

A \mathbb{Z} -biorientation is a weighted biorientation with weights in \mathbb{N}^+ for ingoing halfedges and weights in $\mathbb{Z} \setminus \mathbb{N}^+$ for outgoing half-edges, i.e., ingoing half-edges have strictly positive integer weights, while outgoing half-edges have non-positive integer weights. An \mathbb{N} -biorientation is a \mathbb{Z} -biorientation with outgoing half-edges having weight 0.

Remark 3.2.17: Ordinary orientations correspond to N-orientations, where each edge is 1way with weight 1. More generally, k-fractional orientations are N-orientations where each edge has weight k.

Definition 3.2.18: Let M be a \mathbb{Z} -biorientation with a root face. M is called admissible if the contour of the root face is a simple clockwise cycle of 1-way edges with weights 0 on each outgoing half-edge and weight 1 on each ingoing half-edge, and every inner half-edge incident to an outer vertex is outgoing. M is called **suitable** if it is minimal, admissible, and accessible from every vertex of the root face. We denote by $\tilde{\mathcal{O}}$ the set of suitable \mathbb{Z} -biorientations.

Definition 3.2.19: A mobile is a plane tree with vertices colored either black or white, where each black vertex can be incident to some dangling half-edges called **buds**. The excess of a mobile is the total number of half-edges incident to all white vertices minus the total number of buds. A mobile is **weighted** if for each non-bud half-edge h a weight $w(h) \in \mathbb{R}$ is associated. The **in-degree** of a vertex is the number of incident non-bud half-edges, the **weight** of a vertex is the sum of weights of the incident non-bud half-edges. The out-degree of a black vertex is the number of incident buds, and its degree is the sum of in-degree and out-degree.

A \mathbb{Z} -mobile is a mobile with weights in \mathbb{N}^+ for (non-bud) half-edges incident to a white vertex and weights in $\mathbb{Z} \setminus \mathbb{N}^+$ for (non-bud) half-edges incident to a black vertex.

We now define one of the main mappings on bioriented plane maps as introduced in [BF11], also called "master bijection". The mapping is based on a local transformation performed on each edge.

Definition 3.2.20: Let M be a face-rooted map endowed with a weighted biorientation. We define a **local transformation** as follows:

Let h, h' be the half-edges of an edge e with respective weights w and w'. Let v, v' be the incident vertices, let c, c' be the corners preceding h, h' in clockwise order around v, v', and let f, f' be the faces incident to these corners. Let b_f be a black vertex placed inside each face f of the map.

- 1. If e is 0-way, then create an edge across e connecting the black vertices b_f and $b_{f'}$. Give weight w and w' to the new half-edges. Finally, delete the edge e.
- 2. If e is 1-way with h being the ingoing half-edge, then create an edge connecting the black vertex b_f with the white vertex v in the corner c. Give weight w and w' to the half-edges incident to v and b_f , respectively. Finally, add a bud on $b_{f'}$ in the corner c', and delete the edge e.
- 3. If e is 2-way, then add buds on b_f and $b_{f'}$ in the corners c and c', respectively.

Figure 3.15 illustrates all local transformations, with the respective weights omitted for clarity.

Definition 3.2.21: Let M be a face-rooted map with root face f_0 endowed with a (weighted) biorientation. We view the vertices of M as white and in every face f of M we place a black vertex b_f .

For M in \mathcal{O} , the embedded graph $\Phi(M)$ with black and white vertices is obtained in three steps.

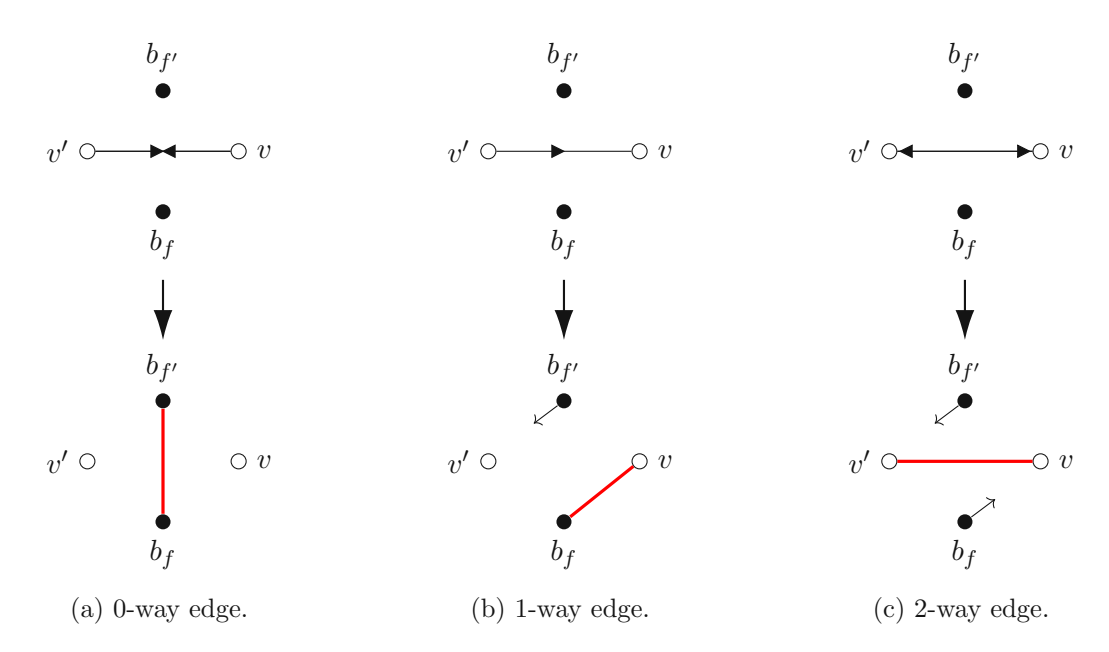


Figure 3.15: Local transformation illustrated without weights.

- 1. Reverse the orientation of all edges of the root face.
- 2. Perform the local transformation of each edge as in Definition 3.2.20.
- 3. Delete the black vertex b_{f_0} and the vertices and edges incident to the root face (after Step 2, no other edge or bud is incident to these outer vertices).

In Figure 3.16, the mapping Φ applied to a biorientation can be seen. In the second subfigure, we show Step 2 of performing all local transformations but keeping edges of the original map for better illustration.

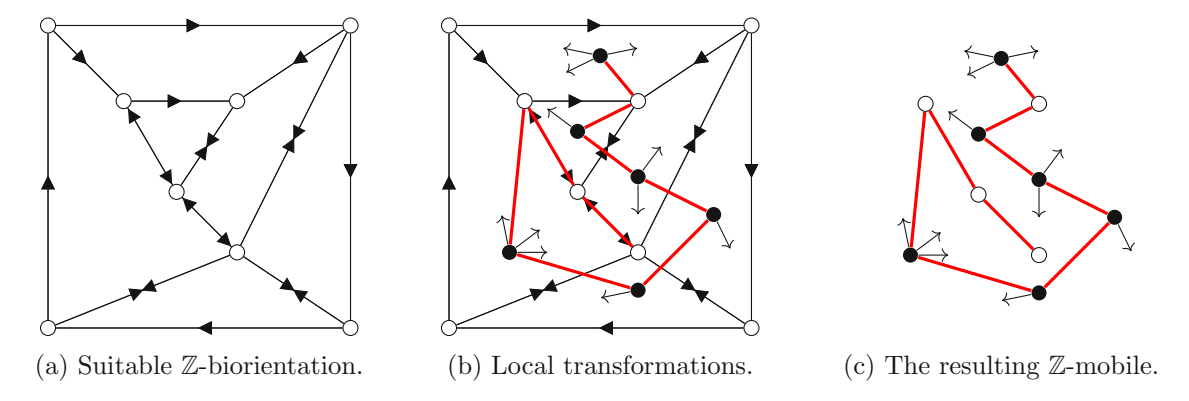


Figure 3.16: The bijection Φ applied to a suitable \mathbb{Z} -biorientation.

One can readily verify that Φ maps any suitable \mathbb{Z} -biorientation to a \mathbb{Z} -mobile of negative excess. By construction of the local transformations, the following parameter correspondences hold between a map M and its associated mobile $\Phi(M)$.

- 1. The outer degree d corresponds to the excess -d;
- 2. inner vertices correspond to white vertices (with the same weight);
- 3. inner faces correspond to black vertices (with the same degree and weight);
- 4. 0-way edges, inner 1-way edges, and 2-way edges correspond to black-black edges, black-white edges and white-white edges (with the same weight).

Example 3.2.22: We explicitly give the parameter correspondences for the Z-biorientation M and its resulting \mathbb{Z} -mobile $\Phi(M)$ in Figure 3.16.

- 1. M has outer degree 4, $\Phi(M)$ has excess 7-11=-4;
- 2. M has 4 inner vertices, $\Phi(M)$ has 4 white vertices;
- 3. M has 6 inner faces, $\Phi(M)$ has 6 black vertices and the degree of each face is equal to the degree of the corresponding black vertex;
- 4. M has 4 0-way edges, 3 inner 1-way edges, and 2 2-way edges, $\Phi(M)$ has 4 black-black edges, 3 black-white edges, and 2 white-white edges.

The mapping Φ can be shown to be a bijection. Although we do not provide the full proof here, we describe how to recover any \mathbb{Z} -biorientation M from its associated mobile $\Phi(M)$.

We first need to introduce a generalized version of the dual of a map.

Definition 3.2.23: Let M be a \mathbb{Z} -orientation. The **oriented dual** M^* of M is obtained by first taking the dual of the map M, disregarding the orientation. Each dual edge e^* corresponding to an edge e of M is then oriented as follows:

- 1. If e is 0-way, e^* is oriented 2-way.
- 2. If e is 2-way, e^* is oriented 0-way.
- 3. If e is 1-way (with the face on its left called f), e^* is oriented 1-way toward the vertex f^* corresponding to f.

Unlike in the non-oriented case, the oriented dual is not an involution: applying it twice yields $(M^*)^*$, which is the original \mathbb{Z} -orientation M with reversed orientations of all 1-way edges. Consequently, the oriented dual is of order 4.

For Algorithm 7, recall the definition of a local closure in Section 3.1 In this case, the local closure is performed counterclockwise, and the newly created edges are 1-way oriented from bud to stem. The definition of a partial closure follows analogously as in the case of blossoming maps.

In [BF11], this construction of a "closure" is introduced for (properly bicolored) mobiles and suitable orientations. Our algorithm extends this construction to \mathbb{Z} -biorientations, and we therefore state the result in a more general form.

```
Algorithm 7 Closing of a \mathbb{Z}-mobile
Require: T a \mathbb{Z}-mobile (possibly weighted) with negative excess \delta
 1: insert a black vertex in the middle of each white-white edge
 2: for e black-white edge do
        x \leftarrow \text{the black vertex of } e
        c \leftarrow the corner incident to x that has e on its right
 4:
        add a stem (ingoing dangling half-edge) at c
 6: end for
 7: perform the partial closure
 8: add a black root vertex v_0 in the outer face
 9: for b unmatched bud do
                                                                           \triangleright there are exactly |\delta|
10:
       substitute b by a 1-way edge from v_0 to b
11: end for
12: delete all white-white and black-white edges and white vertices
13: for v black vertex inserted in line 1 do
14:
        substitute v and its two ingoing edges by a 0-way edge
15: end for
16: for e edge without an orientation do
        orient e as a 2-way edge
17:
18: end for
19: M^* \leftarrow oriented dual of the map M
```

Theorem 3.2.24 ([BF11], Theorem 31.): For any $d \in \mathbb{N}^+$, the closure maps a mobile of excess -d to a suitable biorientation of outer degree d. For any bioriented map M, the closure of $\Phi(M)$ recovers the original map M.

This theorem is the main step in proving that Φ is a bijection.

Theorem 3.2.25: [[BF11], Theorem 11.] The mapping Φ is a bijection between the set $\tilde{\mathcal{O}}$ of suitable \mathbb{Z} -biorientations and the set of \mathbb{Z} -mobiles of negative excess.

Note that in [BF11], the mapping Φ is called Φ_{-} and Theorem 3.2.25 is stated for Nbiorientations and N-mobiles. However, the argument applies analogously when replacing \mathbb{N} with \mathbb{Z} , since the proof does not rely on the non-negativity of weights.

3.2.4 p-gonal d-angulations

20: return M^*

For $p \geq d \geq 3$, we denote by \mathcal{C}_d the class of d-angulations of girth d, and by $\mathcal{C}_{p,d}$) the class of (p-gonal) d-angulations of girth d. For these classes of maps, there is a canonical way to orient each map in \mathcal{C} , thereby associating to \mathcal{C} a corresponding set of oriented maps $\mathcal{O}_{\mathcal{C}}$. By specializing the master bijection of [BF11], we obtain, for each class \mathcal{C}_d (resp. $\mathcal{C}_{p,d}$), a bijection with a class of mobiles characterized by specific degree conditions.

Note that this strategy unifies the bijections for the class C_3 of simple triangulations [FPS08] and the class C_4 of simple quadrangulations [Sch98].



We now introduce a new type of weighted biorientations, closely related to the j/korientations defined in Subsection 3.1.4.

Definition 3.2.26: Let M be a map with a root face of outer degree d with no face of degree less than d. A **pseudo-**d/(d-2)-biorientation of M is an admissible \mathbb{Z} -biorientation such that every outgoing half-edge has weight in $\{0, -1, -2\}$, and

- (i) each inner edge has weight d-2,
- (ii) each inner vertex has weight d,
- (iii) each inner face f has degree and weight satisfying deg(f) + w(f) = d.

For d-angulations, condition (iii) implies that w(f) = 0 for every face f and therefore outgoing half-edges have weight 0. In that case, we refer to the orientation as d/(d-2)biorientation.

The left subfigure of Figure 3.17 shows a 5-angulation M with a suitable (5/3)-biorientation. Since outgoing half-edges have weight 0, the ingoing half-edges of 1-way edges always have weight 3. Therefore, we do not denote the weights for 1-way edges in the illustration. The fact that M is of girth 5, is an example of an important property. Analogously to Subsection 3.1.4, (pseudo-)d/(d-2)-biorientations characterize a certain class of maps, as shown in Section 8.3 of [BF12].

Theorem 3.2.27 ([BF12], Theorem 12): Let M be a map with a root face of outer degree d with no face of degree less than d. Then, M admits a (pseudo-)d/(d-2)-biorientation if and only if M has girth d. In this case, there exists a unique suitable (pseudo-)d/(d-2)biorientation of M.

In particular, Theorem 3.2.27 implies that the class C_d of d-angulations of girth d can be identified with the subset \mathcal{E}_d of \mathbb{Z} -orientations in \mathcal{O} having only faces of degree d, inner edges with weight d-2 and inner vertices of weight d.

For the application of the master bijection, we define a new kind of mobiles.

Definition 3.2.28: A pseudo-d-branching mobile is a Z-mobile such that every halfedge incident to black vertices has weight in $\{0, -1, -2\}$, and

- (i) each edge has weight d-2,
- (ii) each white vertex has weight d,
- (iii) each black vertex v has degree and weight satisfying deg(v) + w(v) = d.

If we additionally demand w(v) = d for every black vertex v, we refer to the mobile as d-branching mobile.

An example of a 5-branching mobile is illustrated in the right subfigure of Figure 3.17. Combining Theorem 3.2.25 with the parameter correspondences listed earlier, one sees that the master bijection Φ maps any \mathbb{Z} -biorientation $M \in \mathcal{E}_d$ to a d-branching mobile of

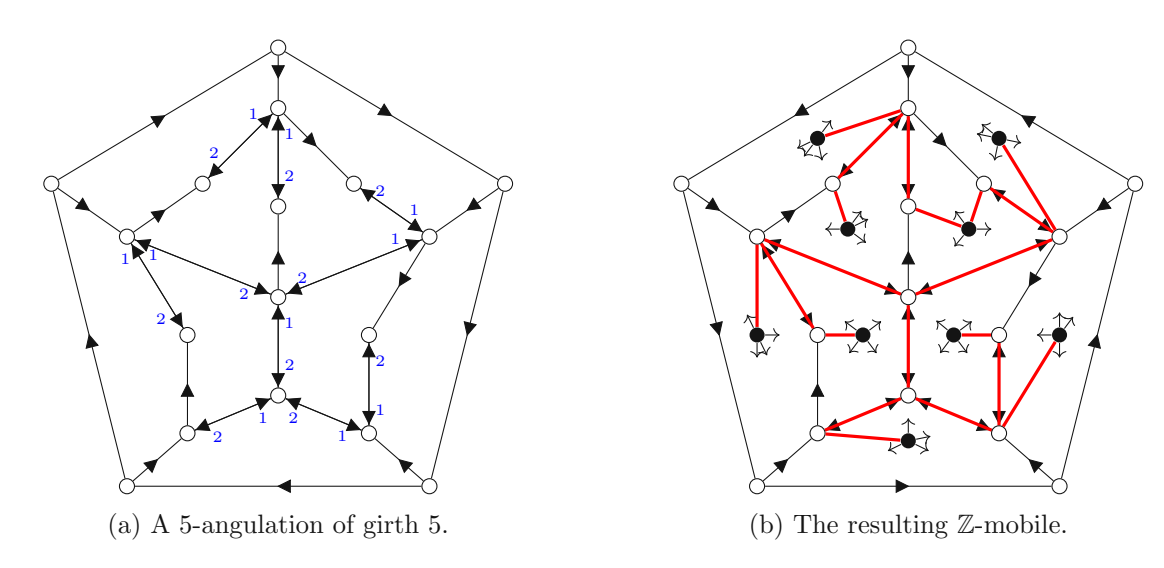


Figure 3.17: A 5-angulation of girth 5 and the 5-branching mobile.

excess -d, and conversely. Moreover, each inner face of M corresponds to a black vertex of the *d*-branching mobile.

The condition of having excess -d is in fact inherent to the class of d-branching mobiles. It follows directly from the degree constraints on black vertices and the weight constraints on white vertices, as a straightforward algebraic consequence. Thus, the master bijection Φ induces a new bijection.

Theorem 3.2.29: For $d \geq 3$ and $n \geq 1$, there is a bijection between the class $\mathcal{C}_d^{(n)}$ of face-rooted d-angulations of girth d with n inner faces and the class of d-branching mobiles with n black vertices.

In Subsection 3.1.4 we did not just find a bijection between d-angulations and a certain class of blossoming trees, but we also managed to generalize this to p-gonal d-angulations with an additionally marked face of degree p with $3 \le d \le p$.

A similar generalization is possible in this case in order to find a bijection between so called **non-separated p-gonal d-angulations** of girth d with n inner faces and so called (p,d)-branching mobiles with n black vertices. We refer to [BF11] for a precise description of this generalization.

3.2.5 Maps of girth d with root face degree d

In [BF12], the master bijection introduced in the previous subsection is extended to yield a correspondence between plane maps of girth d with root face degree d and a family of decorated plane trees called d-branching mobiles.

Definition 3.2.30: For $d \in \mathbb{N}^+$, we consider the class \mathcal{P}_d of face-rooted maps of outer degree d and girth d.

As in the previous section, we first characterize the maps in \mathcal{P}_d via suitable \mathbb{Z} -biorientations, thereby identifying \mathcal{P}_d with a subset of \mathcal{O} . This gives us the possibility to apply the master

bijection to this class of biorientations and obtain a specialized bijection for the maps in

We recall Theorem 3.2.27 and identify the class \mathcal{P}_d with the class \mathcal{F}_d of suitable pseudod/(d-2)-biorientations.

The left side of Figure 3.18 depicts an example for d = 3, i.e., a map with a triangular outer face and girth three, endowed with its suitable 3/1-biorientation.

We apply the master bijection of Theorem 3.2.25 to suitable pseudo-d/(d-2)-orientations \mathcal{F}_d as a subset of $\tilde{\mathcal{O}}$ in full analogy to the construction in the previous subsection.

As before, every pseudo-d-branching mobile has excess -d, so we can immediately conclude the following generalization of the bijective Theorem 3.2.29.

Corollary 3.2.31: For $d \geq 3$, there is a bijection between the class \mathcal{P}_d of face-rooted maps of girth d and outer degree d and the class of pseudo-d-branching mobiles. Each inner face of degree $i \geq d$ in the map corresponds to a black vertex of degree i in the mobile.

Figure 3.18 illustrates the bijection for d=3, showing the correspondence between a suitable pseudo-3/(1)-biorientation and a pseudo-3-branching mobile. For improved readability, we denote positive weights in blue and the absolute value of negative weights in red.

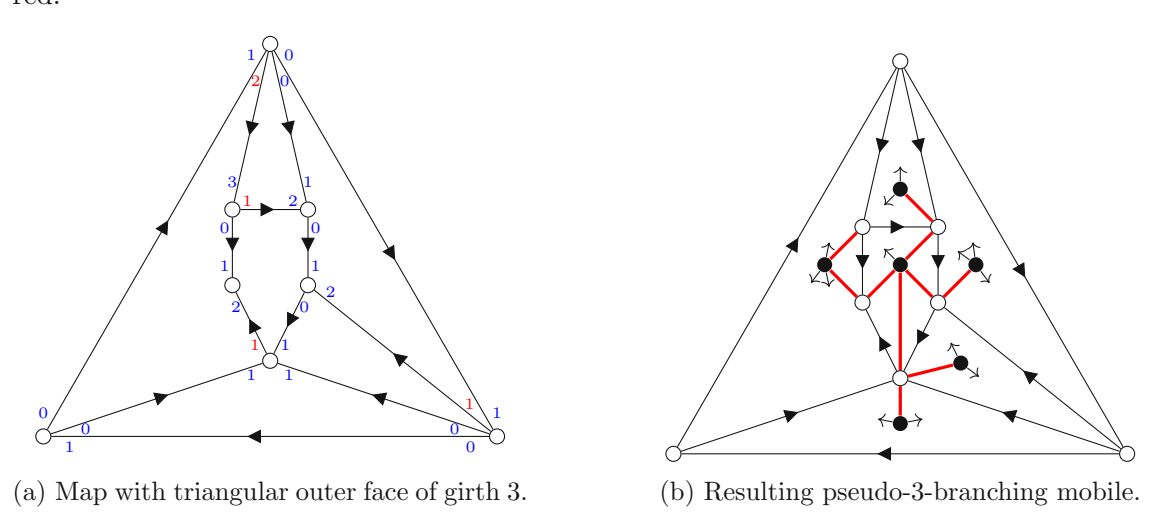


Figure 3.18: A map of girth 3 and the pseudo-3-branching mobile.

3.2.6 Generalization to maps of higher genus

Similar to Subsection 3.1.5, we provide a compact overview of key generalizations of bijections of category (B) for planar maps to maps on surfaces of higher genus.

The CVS bijection has been extended to maps on orientable surfaces of arbitrary genus [MS01; CMS08], while a generalized BDG bijection is constructed for Eulerian maps on orientable surfaces of genus q with a distinguished vertex, leading to so-called q-mobiles [Cha08].

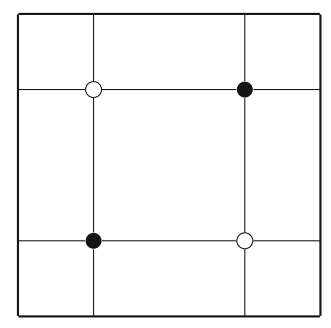


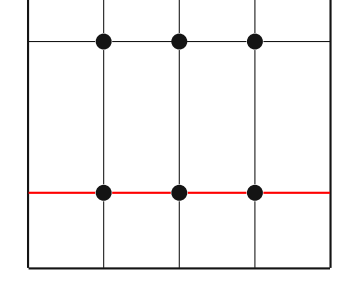
For this subsection, we adopt the definitions from Subsection 3.1.5 about blossoming bijections on higher genus maps. For the following, we define the generalization of plane trees.

Definition 3.2.32: For $g \in \mathbb{N}$, a g-tree is a map of genus g with only one face. A g-tree with a root vertex is called **well-labeled** if each node carries a positive integer label, labels of two adjacent vertices differ by at most 1, and the root node has label 1.

For g = 0, a g-tree is a plane tree; for $g \ge 1$, any g-tree contains at least one cycle.

Recall the CVS bijection Φ from Subsection 3.2.1 between planar quadrangulations and well-labeled trees. One main consideration in the construction of Φ was the fact that the faces of a planar quadrangulation are either simple or confluent since each planar quadrangulation is bipartite. In higher genus, this property no longer holds in general (see the discussion following Lemma 2.1.22). In Subfigure 3.19b, we construct a quadrangulation of genus 1 on the torus that is not bipartite. This can be seen by looking at the cycle of odd length 3, highlighted in red. Bipartite quadrangulations, however, do exist on the torus, as shown in Subfigure 3.19a.





(a) Bipartite quadrangulation.

(b) Non-bipartite quadrangulation.

Figure 3.19: A (non-)bipartite quadrangulation on the torus.

The generalization of the CVS bijection in [CMS08] applies specifically to those bipartite quadrangulations on orientable surfaces of arbitrary genus. When the vertices of a bipartite quadrangulation are labeled with their geodesic distance, each face is either simple or confluent, allowing the local operations defined in Definition 3.2.3 to be applied.

The **opening** Φ_g is defined analogously to the planar case, and the argument that this mapping produces a g-tree follows similarly via the dual exploration graph (DEG). However, For q > 1, one must additionally verify that the unique face of the resulting embedding is simply connected. This is done in [CMS08] using the duality with the DEG and some familiarity with graphs on surfaces, and we omit these technical details here.

The closure of well-labeled g-trees is a natural extension of the construction for welllabeled-trees in the planar case. It can be shown that the closure produces a bipartite quadrangulation of genus q, and together with the opening, it establishes the main bijective correspondence.

Theorem 3.2.33 ([CMS08], Theorem 1): The mapping Φ_q is a bijection from pointed bipartite quadrangulations of genus g with n faces to well-labeled g-trees with n edges.

There also exists an alternative formulation of the bijection, where the pointing of the quadrangulation is exchanged by a rooting, and the q-trees are now rooted.

Corollary 3.2.34 ([CMS08], Corollary 1): The mapping Φ_q can be extended to a bijection from rooted bipartite quadrangulations of genus g with n faces to rooted well-labeled g-trees with n edges.

In [CD17], the Marcus-Schaeffer construction is generalized to include all surfaces, whether orientable or non-orientable. For any surface S, there exists a bijection between rooted bipartite quadrangulations on S and labeled unicellular maps on S.

This extension is especially significant for non-orientable surfaces, for which no bijective tools previously existed to analyze distance properties of random maps.

In the orientable case, the Marcus-Schaeffer bijection relies crucially on a global orientation of the surface (given by the orientation of the root corner), which determines the local opening operations for confluent faces. In the non-orientable case, such a global orientation does not exist. For example, in the rooted bipartite quadrangulation of the Klein bottle \mathcal{N}_1^6 shown in Subfigure 3.20a, the faces lack a consistent notion of clockwise direction, preventing a direct application of the local operations. The construction in [CD17] overcomes this issue by assigning a canonical local orientation to each face prior to applying the operations.

Recall from Subsection 3.2.1 that, in the orientable setting, the dual exploration graph (DEG) was used in the proof that the opening mapping Φ produces a valid map. In the non-orientable setting, the DEG is first constructed using only local orientations, before building the corresponding unicellular map. This order is necessary because, unlike in the orientable case, the orientation of DEG edges cannot be defined from a missing global orientation.

For a given rooted bipartite quadrangulation M on the Klein bottle as shown in Subfigure 3.20a, the corresponding dual exploration graph (DEG) is depicted in Subfigure 3.20b. The construction of the DEG follows the procedure described in [CD17]. We refer to the original source for the proof that this construction is well-defined. In Algorithm 8, we will also denote this construction of a DEG by $\nabla(M)$.

In the algorithm, we refer to the two configurations of faces in Figure 3.12. It can be shown that each face of $M \cup \nabla(M)$ has exactly one of the two given forms (without the red edge); thus, this step is well-defined.

The construction of the map $\Phi(M)$, obtained from the superimposition of the quadrangulation M and its DEG on the Klein bottle, is shown in 3.20c.

Analogously to the orientable case, one can define an inverse mapping Λ on rooted unicellular maps. Given such a map U, the construction of the bipartite quadrangulation $M = \Lambda(U)$ (together with its DEG $\nabla(M)$) proceeds via steps mirroring those used for constructing $\nabla(M)$ in Algorithm 8. The mapping Λ is the inverse of Φ .

The following theorem formalizes the bijection and its preservation of structure between distances in the quadrangulation and labels in the unicellular map.

 $^{^6}$ Maps on a Klein bottle can be illustrated inside a square, with the top edge identified with the bottom edge and the left edge identified with the upside-down right edge.

Algorithm 8 Generalized opening of a rooted bipartite quadrangulation Φ

Require: M rooted bipartite quadrangulation on a general surface

- 1: $\nabla(M) \leftarrow \text{the DEG of } M$
- 2: **for** f face of M **do**
- add a red edge so that the face matches one of the two configurations in Figure 3.12 3:
- 4: end for
- 5: $\Phi(M) \leftarrow$ the map with all vertices of M and red edges
- 6: delete v_0 from $\Phi(M)$
- 7: $e_0 \leftarrow$ the root edge of M
- 8: $c \leftarrow$ the unique corner in $\Phi(M)$ of label 1 that is incident to e_0
- 9: set c to be the root corner of $\Phi(M)$
- 10: **return** $\Phi(M)$

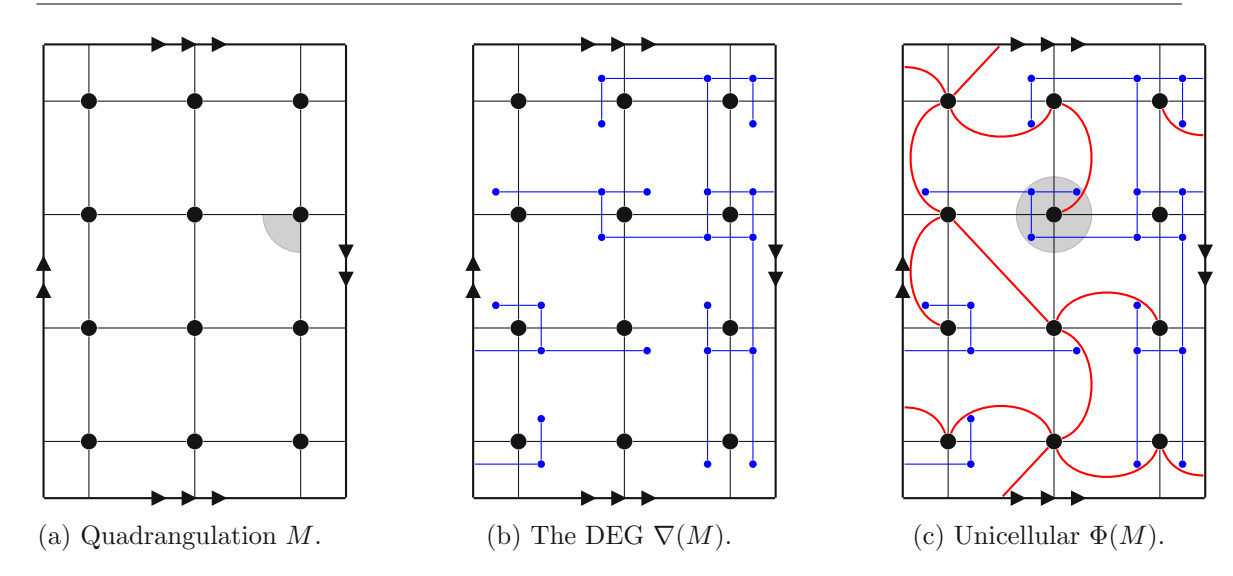


Figure 3.20: The CVS bijection on the Klein bottle.

Theorem 3.2.35 ([CD17], Theorem 3.1): For any surface \mathbb{S} , the mapping Φ is a bijection between the set of rooted bipartite quadrangulations on S with n faces and the set of welllabeled unicellular maps on \mathbb{S} with n edges. Its inverse is given by Λ .

Moreover, if for a given bipartite quadrangulation we denote by N_i the set of its vertices at distance i from the root vertex, and by $E(N_i, N_{i-1})$ the set of edges between N_i and N_{i-1} , then the associated well-labeled unicellular map has $|N_i|$ vertices of label i and $|E(N_i, N_{i-1})|$ corners of label i.



Selected proofs

In this chapter, we prove some selected results from Chapter 3 that are not only crucial for understanding the essential underlying concepts of the bijections, but also yield interesting insights for further study of the topic.

4.1 Proof of the CVS Bijection

Because the CVS bijection serves as a basis for many other constructions, we present here a detailed proof of the intermediate results that lead to the main bijective Theorem 3.2.9. Our proof follows a combination of the ideas of [CS02] and [CMS08].

First, we show some helpful results on the opening Φ .

Lemma 4.1.1: If there exists a cycle in the DEG, it is directed and cycles counterclockwise around a single vertex.

Proof. By definition, each vertex of the DEG has exactly one outgoing edge, so any cycle must be a directed cycle. Moreover, since each vertex also has at least one ingoing edge, the presence of any other vertex inside a cycle of the DEG would force a vertex on the cycle to have two outgoing edges, which is impossible by definition. Thus, the interior of the cycle corresponds to a face in the DEG and contains exactly one vertex of the original quadrangulation. From the definition of the local configurations in Figure 3.12, it follows that the edges of the cycle are counterclockwise around this vertex.

Lemma 4.1.2: The DEG of a quadrangulation with root vertex v_0 contains exactly one (directed) cycle. This cycle encircles the vertex v_0 and can be contracted into a single vertex within the DEG. The resulting contracted DEG is a tree.

Proof. Each edge incident to v_0 induces an edge in the DEG, which is, by definition, oriented such that v_0 is on its right. Thus, these edges form a counterclockwise cycle of the DEG around v_0 .

Given any directed cycle of the DEG, by Lemma 4.1.1, it cycles around a single vertex v. Since each neighbor of this vertex v must have a larger label, this vertex has to be v_0 .

Therefore, the only directed cycle surrounds v_0 . Contracting this cycle in the DEG yields an acyclic connected graph, i.e., a tree.

Theorem 4.1.3: The mapping Φ maps a rooted quadrangulation with n faces to a welllabeled tree with n edges.

Proof. We already know that the resulting map is a tree. In the construction of the mapping, each of the n faces creates a distinct edge of the tree $\Phi(M)$. By definition, each such edge connects two vertices whose labels differ by at most one, so $\Phi(M)$ is also welllabeled.

We now turn to the closing of Algorithm 4 and analyze various of its properties in order to show that it is the inverse of the mapping Φ .

Lemma 4.1.4: In Algorithm 4, the chords of type $\{i, s(i)\}$ can be drawn in a non-intersecting way.

Proof. Let k denote the number of faces of T_0 , and consider any of the k faces. Note that a corner j with i < j < s(i) cannot have a label lower than $l_{s(i)}$, since neighboring corners can only differ by at most one. By the definition of the successor function, the labels of jand s(i) can also not be equal, and therefore we get $l_j > l_{s(i)}$. Assume that there are two chords $\{i, s(i)\}\$ and $\{j, s(j)\}\$ that intersect (w.l.o.g. i < j). This induces a counterclockwise order of these four corners i < j < s(i) < s(j). The first two inequalities imply $l_j > l_{s(i)}$, the last two inequalities imply $l_{s(i)} > l_{s(j)} \ge l_j$, which is a contradiction.

Lemma 4.1.5: After adding chords according to the successor function in Algorithm 4, every face is either triangular with labels l, l+1, l+1 or quadrangular with labels l-1, l, l+1, l. Thus, after the final step of deleting all edges, whose endpoints have equal label, all faces are quadrangular.

Proof. Let F be any of the k faces of T_0 . When adding chords, F is divided by the chords into various smaller faces. Let f be one of those faces and consider the numbers and labels of its corners inherited from F. Let j be the corner in f with the largest number and let i_1 resp. i_2 be the corner following, resp. preceding in clockwise direction, then we have $i_1 < i_2 < j$.

We now distinguish two cases. For the first case, let j be the corner incident to v_0 . Then both its incident corners have label 1 and thus $l_{i_1} = l_{i_2}$.

If j is not incident to v_0 , the edge $\{i_1, j\}$ has to be a chord with $j = s(i_1)$ (and $l_{i_1} = l_j + 1$); if the edge $\{i_1, j\}$ was not a chord, we would have $i_1 = j + 1$ contradicting the maximality of j. Since i_2 lies on the clockwise tour around the face f from i_1 to j, its label cannot be smaller than l_{i_1} due to the definition of $j = s(i_1)$. Together with the fact that the labels of neighboring corners can differ by at most one and hence $l_{i_2} \leq l_j + 1$, we also get the equality $l_{i_2} = l_{i_1} = l_j + 1$ in this case.

As a next step, we show that the edge $\{i_1, i_1 + 1\}$ borders the face f. If not, there would need to be a chord arriving at the corner of i_1 between this edge and the chord $\{i_1, j\}$. By construction of the successor function, this chord would have to come from a corner i_3 with $i_1 < i_3 < j$, and would thus intersect the chord $\{i_1, j\}$, which contradicts the result of Lemma 4.1.4.

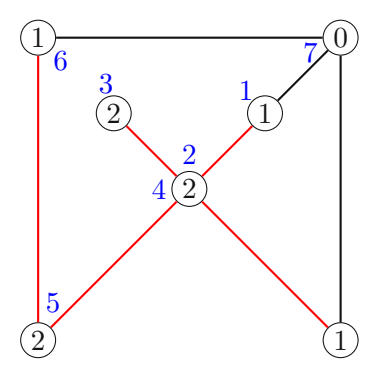
As mentioned above, the label of a corner in the clockwise tour around the face f from i_1 to j cannot be smaller than l_{i_1} . Due to this consideration, as a neighboring corner, there are only two possibilities for the label of $i_1 + 1$:

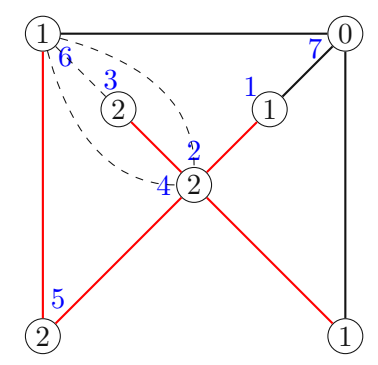
- 1. $l_{i_1+1} = l_{i_1}$, then $i_1 + 1$ cannot be different from i_2 since otherwise, there would be a chord $\{i_1+1,j\}$ excluding i_2 from the face f. Thus, the face f is triangular.
- 2. $l_{i_1+1} = l_{i_1} + 1$, then $i_1 + 1$ is connected to i_2 because i_2 is its successor. If there were another corner $i_3 < i_2$ with $i_3 = s(i_1)$, and a chord $\{i_3, j\}$ would exclude i_2 from the face f. Thus, the face f is quadrangular.



In summary, any edge whose endpoints have the same label l is adjacent to two triangular faces, each having a third vertex of label l-1. Removing such an edge in the last step merges these two triangles into a (simple) quadrangular face with the desired label pattern, completing the proof.

Figure 4.1 shows an illustration that can be very helpful in understanding the proof.





- (a) Step 1 applied to a well-labeled tree. Corners of the face F are numbered in blue.
- (b) Adding chords to the face F. Added chords illustrated in dashed lines.

Figure 4.1: Illustration for understanding the proof of Lemma 4.1.5. Consider the face f_1 with j = 7 and $i_1 = 1, i_2 = 6$ as an example for a quadrangular face and the face f_2 with j = 6 and $i_1 = 4$, $i_2 = 5$ as an example for a triangular face.

As a next step, we show a statement about the number of faces that the resulting quadrangulation has.

Lemma 4.1.6: Let T be a well-labeled tree with n edges. Applying the closing procedure to T produces a quadrangulation with n faces.

Proof. A tree with n edges has n+1 vertices. In the first step of Algorithm 4, another vertex v_0 is added and thus, by the previous lemma, a quadrangulation Q with n+2vertices is obtained in the following steps. We call f the number of faces; since each face of a quadrangulation has degree 4 and each edge is incident to exactly two faces, the number of faces must equal 4m/2 = 2m. Using Euler's formula, we obtain the equation (n+2)-2m+m=2 and simplify it for m=n.

We have shown so far that the mapping $\Phi: \mathcal{Q}_n \to \mathcal{W}_n$ and the closing procedure $\Psi: \mathcal{W}_n \to \mathcal{Q}_n$ can be applied one after another due to their domain and co-domain. It remains to be shown that both mappings are inverse to each other.

Theorem 4.1.7 ([CS02], Proposition 2): The closing procedure is the inverse of the mapping Φ .

Proof. Since the rooting conventions of Φ and Ψ agree in straightforward manner, we omit further discussion of them.

For a given well-labeled tree T, the faces of the map T' obtained after adding all chords are classified as in Lemma 4.1.5. As can be seen in the proof of the lemma, each face of T'

is bordered by the edge $\{i_1, i_1 + 1\}$ which is also part of the original tree. For a triangular face (and its corresponding incident triangular face with the same label distribution), this boundary edge $\{i_1, i_1 + 1\}$ is precisely the one removed during the opening step, ensuring that the face merges correctly into a simple quadrangular face. For a (confluent) quadrangular face, this is exactly the edge that is chosen for a local operation. Thus, applying the local operations to the closing $\Psi(T)$ selects exactly the n edges of the original tree, and we have $\Phi(\Psi(T)) = T$.

For our bijective result, it remains to show that $\Psi(\Phi(Q)) = Q$ for any given quadrangulation Q. From now on, we call $T = \Phi(Q)$ the corresponding tree and Q' the map obtained after performing a local operation (and hence adding a diagonal edge) to each simple face. Applying the mapping Ψ to T, we call T_0 and T' the two maps obtained after Step 2 and Step 3. We will first prove that T' = Q'. The equality $\Psi(\Phi(Q)) = Q$ follows directly, since Q' is obtained from Q by adding diagonal edges in simple faces, and $\Psi(T)$ is obtained from T' by removing exactly those edges producing simple quadrangular faces (see the proof of Lemma 4.1.5).

Consider the root vertex v_0 of Q resp. Q' and the local transformations around it to construct $T = \Phi(Q)$. Each edge with labels 1-2 in T has been part of a confluent face in Q and is thus on the left side of a corner in Q' that has an edge with labels 1-0 on its right side. Each edge with labels 1-1 in T has been part of a simple face in Q and is thus part of two such corners in Q'. Hence, the map T_0 produced by Step 1 of the closing procedure Ψ , where an edge with labels 1-0 is added to each corner of label 1, is not only a submap of T' but also a submap of Q'.

Moreover, T_0 covers all the vertices of T, so that edges of T' not in T_0 are edges in the faces of T_0 . The same holds for T_0 as a submap of Q'. Note that T' and Q' have the same number of vertices and, by Lemma 4.1.5, also the same number of triangular and quadrangular faces. Thus, we can conclude by Euler's formula that they must have the same number of edges. By this consideration, it is enough to show that for each face of T_0 , each chord of T' is also an edge of Q' (by the equality of the numbers of edges, the opposite inclusion is not necessary) to finally show T' = Q'.

Let now f be a face of T_0 . By construction, the face contains exactly one corner of label 0 and two neighboring corners of label 1. For the case deg(f) = 3, these are the only three corners; for the case $\deg(f) = 4$, there exists another corner that must be of label 2, since labels along the border can only differ by ± 1 . In both cases, no chord is added inside the face during the construction of T', and there is no other edge inside the face of Q'. Thus, we now assume $k := \deg(f) \geq 5$ and number the corners (and thus the vertices) of the face in clockwise order from 1 to k starting from the corner after the one incident to the root vertex. By e_i we denote the label of the corner with number i. Note that $e_1 = 1, e_2 = 2, e_{k-2} = 2, e_{k-1} = 1, e_k = 0$, and $e_i \ge 2$ otherwise. We consider the corners with label 2 in increasing order with numbers $i_1 = 2 < i_2 < \dots i_p = k-2$. By the definition of the successor function, for each $1 \leq j < p$, the chord $\{i_j, k-1\}$ is added for the creation of T'. In the following, we will check inductively that these edges also appear in Q'. Firstly, for the chord $\{i_1, k-1\}$ in T', we consider in Q' the face f_1 that contains the corners with labels 0, 1 and 1 (with numbers k, 1 and k-1). Since f has degree larger than 4, also f_1 cannot be triangular and must contain a fourth corner (with label 2). If $i_p = k - 2$ was the fourth corner, the corner of the face f_1 would read (k, 1, k - 2, k - 1) in clockwise order, starting with the corner of label 0. In this case, the edge $\{1, k-2\}$ would have been selected for the creation of the tree $\Phi(Q)$, but it is not an edge of T_0 . Thus, the only other possibility of $i_1 = 2$ being the fourth corner of f_1 remains, and we have shown that $\{i_1, k-1\}$ was an edge of Q'.

For the induction step, let now 1 < j < p and assume that $\{i_{j'}, k-1\}$ was an edge of Q' for each j' < j. Consider in Q' and inside of f the face f_j that is incident to the edge $\{i_j-1,i_j\}$. We distinguish two cases. If $e_{i_j-1}=2$, the edge $\{i_j-1,i_j\}$ was added inside a confluent face of Q and thus, the face f_j is triangular and contains the edge $\{i_1, k-1\}$. In the other case, if $e_{i_j-1}=3$, the face f_j is a (simple) quadrangular face and the other edge from i_i goes to a corner of label 1. If this edge connected i_i to the corner with number 1, it would intersect the edge $\{i_1, k-1\}$ by the same argument as in the proof of Lemma 4.1.4. Hence, there must be the edge $\{i_j, k-1\}$ in Q'.

So far we have shown that each chord in T' with labels 1-2 was also an edge in Q'. Adding all of these chords to T_0 yields a new map T_1 in which each face f is subdivided into faces f_i with the following property: Each face f_i obtained at this stage has exactly one corner with label 1 and two neighboring corners with label 2, each other corner has label at least 3 – the same structure as f, except that the minimum label is 1 instead of 0. By subtracting one from all labels, we obtain an isomorphic situation. Thus, we can show that each chord in T' with labels 2-3 was also an edge in Q', create a new map T_2 by adding all these chords to T_1 , and continue this argumentation successively until we are left with $T_{e_{max}} = T'$ (where e_{max} is the maximum label of all corners in T_0). This completes the proof of T' = Q' and thus $\Psi(\Phi(Q)) = Q$.

4.2 Proof of the unified bijective scheme of category (A)

We state and prove a theorem from [AP15] that implies Theorem 3.1.18 and is at the heart of all bijections between orientations on maps and blossoming trees.

Theorem 4.2.1 ([AP15], Theorem 2.3): Let M be a plane map with root vertex v_0 , and suppose that M is endowed with a minimal accessible orientation O. Then M admits a unique edge-partition $(\mathcal{T}_M, \mathcal{C}_M)$ such that:

- 1. edges in \mathcal{T}_M (called **tree edges**) form a spanning tree of M, rooted at v_0 , on which the restriction of O is accessible;
- 2. any edge in C_M (called **closure edges**) is a saturated clockwise edge in the unique cycle it forms with edges in \mathcal{T}_M .

Let us call such a partition a tree-and-closure partition.

Proof. We carry out the proof by induction on the number of faces of M. If M has one face, we take $\mathcal{T}_M := M$ and $\mathcal{C}_M := \{\}$. Thus, \mathcal{T}_M is a spanning tree of M, and it is accessible since M is. This tree-and-closure is unique since the only spanning tree of a tree is the tree

Let now M be a plane map with root vertex v_0 and n faces (with $n \geq 2$) endowed with a minimal accessible orientation O. We assume the existence and uniqueness of a tree-and-closure partition for any such map with less than n faces.

We try to find an edge e whose deletion from M produces a map M' that is still accessible. In this case, e was not a bridge, therefore the map M' has n-1 faces, and we are done because we can simply apply our assumption to the map M' to obtain a tree-and-closure partition $(\mathcal{T}'_M, \mathcal{C}_{M'})$. The partition of M is then given by $(\mathcal{T}'_M, \mathcal{C}_{M'} \cup \{e\})$.

Due to minimality, the outer edges do not form a counterclockwise cycle, thus at least one of them has the outer face on its left and is not a bridge. Let (u, v) be such an edge; if the map is still accessible after deleting (u, v), we can choose e := (u, v) and are done. Otherwise, let

$$A := \{w \in V(M) | v_0 \text{ is accessible from } w \text{ in } M'\}, \quad U := V(M) \setminus A$$

Note that there can be no edge from U to A. It is easy to see that $v \in A$ and $u \in U$. Moreover, for any vertex $w \in U$, accessibility to v_0 in M required the edge (u, v), so u is accessible from each such w. Because (u, v) was not a bridge, there must exist an edge from A to U. Deleting such an edge does not change the accessibility of vertices. Thus, we can choose as the edge e the leftmost of these edges (having the outer face on its left) and apply the same strategy as above. This reduces the number of faces by one, while preserving minimality and accessibility.

To show the uniqueness of this tree-and-closure partition, we assume that there exists another partition $(\mathcal{T}'_M, \mathcal{C}_{M'})$ with the edge e = (x, y) of the previous step in the tree, or equivalently $e \notin \mathcal{C}'_M$. From now on, for vertices u, v, we denote by $\tau_{u,v}$ the directed path from u to v with edges in \mathcal{T}'_M if it exists. Moreover, we simply write $\tau_u := \tau_{u,v_0}$ for the path to the root vertex. Since \mathcal{T}'_M is accessible, there exists such a path τ_u for each vertex u, and this path is uniquely determined as two different paths would create a cycle in the tree. We first note that $\tau_x = \{(x,y)\} \cup \tau_y$. Let π_x denote the path from x to v_0 with edges in \mathcal{T}_M . This path π_x cannot be completely contained in \mathcal{T}_M' , thus it must contain at least one closure edge $e \in \mathcal{C}_M'$.

Let thus $e_1 = (x_1, y_1)$ be the first closure edge in π_x and consider the path τ_{y_1} and the path τ_{x,x_1} . The edge e_1 builds a cycle with edges of the paths τ_{x,x_1} , τ_{y_1} and τ_{x} .

If the involved edges of the path τ_{y_1} had the inside of this cycle on its left, so would the edge e_1 . This is not possible since, by the definition of a closure edge, e_1 is oriented clockwise in the unique cycle it forms with tree edges. Thus, the involved edges of τ_{u_1} have the inside of the cycle on its right. This implies that τ_{y_1} intersects τ_x already at the vertex x since e = (x, y) has the outer face on its left and cannot be "wrapped" by edges of τ_{y_1} .

We can now define π_{y_1} as the intersection of the path π_x that starts at y_1 . The path π_{y_1} has to contain closure edges, too. Otherwise, there would be a cycle $\pi_{y_1} \cup \tau_{y_1}$ of tree edges. Let $e_2 = (x_2, y_2)$ be the first closure edge and show in exactly the same way as before that τ_{y_2} intersects τ_x at x. This yields an infinite strictly nested sequence of closure edges in π_x , which is impossible in a (finite) map. Hence our assumption was false, and the partition is unique.

¹More precisely, the edge $e_1 = (x_1, y_1)$ builds the cycle with the tree edges $\tau_{x,x_1} \cup (\tau_{y_1} \triangle \tau_x)$ since the paths τ_{y_1} and τ_x might intersect (which they do as we show in the course of the proof).

Applications

5.1 Enumeration of Maps

The systematic enumeration of planar maps began in the 1960s with the pioneering work of Tutte [Tut63]. By exploiting recursive decompositions of maps, Tutte derived functional equations satisfied by their generating functions, from which explicit enumeration formulas could be extracted.

Since then, successful ideas have been used to rederive and generalize the results of Tutte, including the bijective constructions presented in this work. These not only provide an elegant rederivation of Tutte's formulas, but also yield deeper insights into the combinatorial structure of maps.

In this section we present enumeration formulas for two classes of planar maps, obtained by analyzing the corresponding classes of decorated trees given by the bijections introduced earlier.

5.1.1 Rooted Eulerian planar maps

We use the bijection between balanced Eulerian blossoming trees and rooted Eulerian planar maps (Theorem 3.1.7) to enumerate the number of rooted Eulerian planar maps and, from these, derive the enumeration of rooted planar maps in general.

We start by stating a classical result about planted plane trees.

Lemma 5.1.1 ([Wal72]): The number of planted plane trees with d_i vertices of degree i+1for $i \ge 1$, $k = 2 + \sum (i+1)d_i$ leaves and $n = (\sum d_i) + k - 1$ edges is

$$\frac{1}{n} \binom{n}{k-1, d_1, d_2, \dots, d_{i_{max}}} = \frac{(n-1)!}{(k-1)!} \prod_{i>1} \frac{1}{d_i!}, \tag{5.1}$$

where i_{max} is the maximal index i such that $d_i \neq 0$.

Recall from Subsection 3.1.1 how marked Eulerian blossoming trees can be obtained from planted plane trees. This connection, together with Formula (5.1), immediately implies the following lemma.

Lemma 5.1.2: The number of marked Eulerian blossoming trees with d_i vertices of degree 2i for $i \ge 1$, k closing stems and n - k edges is

$$\frac{(n-1)!}{(k-1)!} \prod_{i\geq 1} {2i-1 \choose i}^{d_i} \frac{1}{d_i!},\tag{5.2}$$

As a final step, we link this enumeration of marked Eulerian blossoming trees to the enumeration of rooted Eulerian planar maps using the bijective approach.

Proposition 5.1.3: The number of rooted Eulerian planar maps with d_i vertices of degree 2i, e edges and v vertices is

$$\frac{2e!}{(e-v+2)!} \prod_{i>1} {2i-1 \choose i}^{d_i} \frac{1}{d_i!}.$$
 (5.3)

Proof. In an Eulerian blossoming tree, each of the k closing stems can be marked, yielding k pairwise conjugate trees, 2 of which are balanced. If the tree admits a rotational symmetry of order 2, then the conjugacy class has size k/2, and only one balanced tree remains. In both cases, the proportion of balanced trees in a conjugation class of marked Eulerian blossoming trees is 2/k.

Multiplying Formula 5.2 with this factor yields the number of balanced Eulerian blossoming trees

$$2\frac{(n-1)!}{k!} \prod_{i \ge 1} {2i-1 \choose i}^{d_i} \frac{1}{d_i!}.$$

By Theorem 3.1.7, these balanced blossoming trees correspond bijectively to rooted Eulerian planar maps, with the same number of vertices v = n - k + 1 and e = (n - k) + (k - 1) = 0n-1 edges.

As a direct consequence, we obtain an enumeration formula for rooted planar maps, which are in bijection with a special class of rooted Eulerian planar maps.

Corollary 5.1.4: The number of rooted planar maps with m edges is given by

$$\frac{2\cdot 3^m}{(m+2)(m+1)} \binom{2m}{m}.$$

Proof. By the medial map bijection (Lemma 2.1.31), the number of rooted planar maps with m edges equals the number of rooted 4-regular maps with 2m edges (and m vertices). By Formula 5.3 these can be enumerated by

$$\frac{2 \cdot (2m)!}{(m+2)!} {4-1 \choose 2}^m \frac{1}{m!}$$

which simplifies to the claimed expression.

5.1.2 Rooted simple triangulations

Using the bijection of Subsection 3.1.2 between marked triangular blossoming trees and rooted simple triangulations, we derive an enumeration formula for rooted simple triangulations in this subsection.

We first state an auxiliary result as given in [PS06].

Lemma 5.1.5: The number of triangular blossoming trees with n nodes is given by

$$\mathcal{B}_n^{\triangle} = \frac{2}{4n-2} \cdot \binom{4n-2}{n-1}.$$

A triangular blossoming tree with n nodes has 2n opening stems, and exactly two of these can be marked to yield a balanced triangular blossoming tree. Therefore, the ratio of balanced trees in $\mathcal{B}_n^{\triangle}$ is 2/(2n) = 1/n.

Corollary 5.1.6: The number of rooted simple triangulations of size n is given by

$$\mathcal{T}_n = \frac{1}{n(2n-1)} \cdot \binom{4n-2}{n-1}.$$

5.2 Intrinsic geometries of planar quadrangulations and maps

Beyond the combinatorial interpretation of counting formulas, an important motivation for developing the bijective methods is that they are the cornerstone of the study of random

One important motivation from statistical physics is the interpretation of random maps, particularly triangulations and quadrangulations, as discrete models of random surfaces in two-dimensional Euclidean quantum gravity. Using bijective methods, we discuss results concerning the geometry of those random maps. For example, in a random rooted planar quadrangulation with n faces, the typical graph distance between two uniformly chosen vertices is of order $n^{1/4}$ [CS02]. Moreover, uniform random quadrangulations, rescaled by the factor $n^{1/4}$, converge in distribution to the so-called Brownian map [Mie13; Le 13].

The CVS bijection was the starting point for deriving distance properties in random planar maps.

5.2.1 Distances in planar maps

Definition 5.2.1: Let M be a rooted planar map with root vertex v_0 . Then, the radius (sometimes also called **eccentricity**) r of M is defined as the maximum distance from the root vertex $r := \max\{d(v, v_0) : v \in M\}$. For a rooted plane tree T, the radius is called the height H(T).

Let M_n be a random planar quadrangulation that is uniformly distributed in Q_n , the set of planar quadrangulations with n faces. We begin by analyzing the distance from a uniformly chosen vertex to the root vertex. The CVS bijection provides a convenient framework to determine this distance.

Let E_n be a uniform rooted embedded tree with n edges. This random tree E_n can be constructed from a uniform (unlabeled) plane tree T_n by assigning a label increment in $\{-1,0,1\}$ to each edge, chosen uniformly and independently. The label of a vertex is then defined by summing these increments along the path from the root vertex, with the root label set to 0.

It is well known (see, e.g. Section 20.3 in [Jan11]) that the height $H(T_n)$ of a uniform plane tree is typically of order $n^{1/2}$, and the distance from a uniformly chosen vertex of T_n to the root vertex is of the same order. Since the label of a vertex is obtained by summing $\theta(n^{1/2})$ independent, centered, bounded increments, by the central limit theorem, the label is of order $(n^{1/2})^{1/2} = n^{1/4}$ in probability.

Via the CVS correspondence, these labels encode graph distances in M_n . This provides a heuristic explanation for the $n^{1/4}$ scaling of distances in quadrangulations.

We refer to [CS02] for a rigorous analysis of this approach and state a result from the paper.

Theorem 5.2.2 ([CS02], Corollary 3): The random variable $n^{-1/4}r_n$ converges weakly to $(8/9)^{1/4}r$, where r_n is the radius of the quadrangulation corresponding to M_n and $r \geq 0$ is a real-valued random variable.¹

5.2.2 The Brownian map as a universal scaling limit

From the observation of the previous subsection that the distance from a random vertex to the root vertex is typically of order $n^{1/4}$, the idea arises to find a certain kind of continuum limit for random planar quadrangulations of size n rescaled by a factor of order $n^{-1/4}$. In this subsection, we closely follow the presentation of [Le 13] and [Gal14]. We adopt the framework and definitions, restating key theorems as in the original work, while occasionally providing additional explanations for clarity.

Definition 5.2.3: Let (X, d) be a metric space. For $s \ge 0$, $\delta > 0$ and $E \subseteq X$, set

$$\mathcal{H}^{s}_{\delta}(E) = \inf \left\{ \sum_{i=1}^{\infty} \operatorname{diam}(U_{i})^{s} | U_{i} \subseteq X, E \subseteq \bigcup_{i=1}^{\infty} U_{i}, \operatorname{diam}(U_{i}) < \delta \right\},\,$$

where diam $(U) := \sup\{d(x,y) : x,y \in U\}$ for each $\emptyset \neq U \subseteq X$ and diam $(\emptyset) := 0$. Any collection $(U_i)_{i>1}$ from the definition is called a δ -covering of E. The s-dimensional **Hausdorff measure** of E is then defined as

$$\mathcal{H}^s(E) := \lim_{\delta \to 0} \mathcal{H}^s_{\delta}(E).$$

From the definition of the Hausdorff measure, we can immediately show an interesting property.

Lemma 5.2.4: Let (X,d) be a metric space, $s \ge 0, \delta > 0, E \subseteq X$. Then, for every t > s, we have

$$\mathcal{H}_{\delta}^{t}(E) \le \delta^{t-s} \mathcal{H}_{\delta}^{s}(E). \tag{5.4}$$

Proof. Let $(U_i)_{i\geq 1}$ be a δ -covering of E. For any $i\geq 1$, by definition $\operatorname{diam}(U_i)^{t-s}<\delta^{t-s}$, and we get

$$\sum_{i\geq 1} \operatorname{diam}(U_i)^t = \sum_{i\geq 1} \operatorname{diam}(U_i)^{t-s} \operatorname{diam}(U_i)^s < \sum_{i\geq 1} \delta^{t-s} \operatorname{diam}(U_i)^s.$$

Taking the infimum over all δ -coverings of E yields the inequality.

The previous lemma implies another basic result about the Hausdorff measure.

¹ "The random variable r is the radius of the limiting Brownian map; see [CS02] for its definition and exact value.



Proposition 5.2.5: Let (X,d) be a metric space, $E \subseteq X$ and $0 \le s < t$. Then, we have the following properties.

- $\mathcal{H}^s(E) < \infty \implies \mathcal{H}^t(E) = 0$;
- $\mathcal{H}^t(E) > 0 \implies \mathcal{H}^s(E) = \infty$.

Proof. Using the previous lemma, we assume the left side of the implication and get

•
$$\mathcal{H}^t(E) = \lim_{\delta \to 0} \mathcal{H}^t_{\delta}(E) \overset{(5.4)}{\leq} \lim_{\delta \to 0} \delta^{t-s} \mathcal{H}^s_{\delta}(E) = \mathcal{H}^s(E) \cdot \lim_{\delta \to 0} \delta^{t-s} = 0$$

•
$$\mathcal{H}^s(E) = \lim_{\delta \to 0} \mathcal{H}^s_{\delta}(E) \overset{(5.4)}{\geq} \lim_{\delta \to 0} \delta^{s-t} \mathcal{H}^t_{\delta}(E) = \mathcal{H}^t(E) \cdot \lim_{\delta \to 0} \delta^{s-t} = \infty.$$

We can now define the Hausdorff dimension of a subset E as the unique value s along \mathbb{R} , where the measure transitions from being ∞ to being 0 as indicated by the previous proposition.

Definition 5.2.6: Let (X,d) be a metric space. For $E \subseteq X$, the **Hausdorff dimension** of E is defined by

$$\dim_{\mathrm{H}}(E) := \inf\{s \ge 0 : \mathcal{H}^s(E) = 0\} = \sup\{s \ge 0 : \mathcal{H}^s(E) = \infty\}.$$

These notions allow for a description of the "size" of sets in a metric space, extending the idea of integer-valued topological dimension to non-integer values. It can be shown easily that the Hausdorff dimension coincides with the common notion of dimension for shapes of "traditional" geometry. Examples are $\dim_{\mathrm{H}}([0,1])=1$ and $\dim_{\mathrm{H}}([0,1]^2)=2$. On the other hand, for fractal sets non-integer values arise (e.g., the well-known Cantor set has Hausdorff dimension $\log 2/\log 3$).

We consider a random planar quadrangulation M_n that is uniformly distributed in Q_n and identify M_n with the finite metric space $(V(M_n), d_{M_n})$, where d_{M_n} is the graph distance on the vertex set $V(M_n)$. Thus, we can also view M_n as a random variable taking values in the space M of compact metric spaces up to isometry. We want to endow the space M with a topology by defining a distance between two metric spaces.

Definition 5.2.7: A correspondence $\mathcal{R} \subseteq X \times Y$ between two sets X and Y is a relation such that for every $x \in X$, there exists at least one $y \in Y$ with $(x,y) \in \mathcal{R}$ and for every $y' \in Y$, there exists at least one $x' \in X$ with $(x', y') \in \mathcal{R}$. We denote by Cor(X, Y) the set of all correspondences between X and Y.

Let (X, d_X) and (Y, d_Y) be two metric spaces and \mathcal{R} be the correspondence between Xand Y. The **distortion** $dis(\mathcal{R})$ of \mathcal{R} is defined as

$$\operatorname{dis}(\mathcal{R}) := \sup_{(x,y),(x',y')\in\mathcal{R}} |d_X(x,x') - d_Y(y,y')|.$$

Definition 5.2.8: Let (X, d_X) and (Y, d_Y) be two compact metric spaces. The **Gromov-Hausdorff distance** $d_{GH}(X,Y)$ is defined to be

$$d_{GH}(X,Y) := \frac{1}{2} \inf_{\mathcal{R} \in Cor(X,Y)} \operatorname{dis}(\mathcal{R}).$$

Note that this definition of the Gromov-Hausdorff distance is actually a reformulation of another definition that builds on the more familiar Hausdorff distance between sets. The definition presented here turns out to be more useful for explicit computations and concrete examples. In addition, we adopt the convention with the prefactor 1/2; some authors omit it, leading to an equivalent distance up to scaling.

The space (\mathbb{M}, d_{GH}) of compact metric spaces up to isometry, endowed with the Gromov-Hausdorff distance, is a separable and complete metric space. For proofs, see, for example, Theorem 7.3.30 in [BBI01] and Theorem 1 in [EPW04]. Within this space, the scaling limits of random maps can be studied. An important result of [Le 13] shows that for several classes of planar maps, after rescaling the graph distances by a factor of order $n^{-1/4}$, the vertex set converges in distribution to a random compact metric space known as the **Brownian map**. More precisely:

Theorem 5.2.9 ([Le 13], Theorem 1.1): Suppose that either p=3 or $p\geq 4$ is an even integer, set

$$c_p = \left(\frac{9}{p(p-2)}\right)^{1/4}$$

if p is even, and

$$c_3 = 6^{1/4}$$
.

For every integer $n \geq 2$, let \mathcal{M}_n^p denote the set of rooted p-angulations with n faces, let M_n be uniformly distributed over \mathcal{M}_n^p . There exists a random compact metric space $(\boldsymbol{m}_{\infty}, D^*)$ called the Brownian map, which does not depend on p, such that

$$(V(M_n), c_p n^{-1/4}) d_{M_n}) \xrightarrow[n \to \infty]{(d)} (\boldsymbol{m}_{\infty}, D^*)$$
(5.5)

where the convergence holds in distribution with respect to the Gromov-Hausdorff distance

In other words, the Brownian map arises as a universal scaling limit for different classes of planar maps, independent of the face degree parameter p, up to the scaling constant c_p . As a concrete example, for the case of triangulations (p=3), the rescaled vertex set

$$(V(T_n), 6^{1/4}n^{-1/4}d_{T_n})$$

converges in distribution to the Brownian map. The special case of quadrangulations (d=4) was obtained independently in [Mie13]. The theorem illustrates how a highly combinatorial object such as a random triangulation encodes, in the large size limit, a universal continuous random surface.

We now want to precisely construct this limiting space.

The Brownian continuum random tree (CRT) (introduced and studied by Aldous [Ald93]) is another famous probabilistic model that is a universal scaling limit of discrete trees, in a sense analogous to (5.5). The Brownian map can be constructed from the CRT by gluing certain pairs of points.

Our discrete bijections from the previous sections are not able to fully explain the results as (5.5), but they provide a good background for understanding the construction of the Brownian map from the CRT. The underlying idea of the construction of the Brownian map is to use a continuous analog of the CVS bijection, where plane trees will be substituted by Aldous' CRT. A discussion of scaling limits of labeled plane trees can be found in [GM12]. Therefore, we first introduce another well-known random compact space.

Definition 5.2.10: A metric space (\mathcal{T}, d) is called \mathbb{R} -tree if for every $a, b \in \mathcal{T}$

- 1. there exists a unique isometric map $f_{a,b}$ from [0,d(a,b)] into \mathcal{T} such that $f_{a,b}(0)=a$ and $f_{a,b}(d(a,b)) = b$ and
- 2. for a continuous injective map q from [0,1] into \mathcal{T} with q(0)=a and q(1)=b, we have

$$q([0,1]) = f_{a,b}([0,d(a,b)]).$$

The elements of an \mathbb{R} -tree \mathcal{T} are called **vertices**. A vertex $a \in \mathcal{T}$ is called a **leaf** if $\mathcal{T} \setminus \{a\}$ is connected.

If a vertex ρ in an \mathbb{R} -tree is distinguished, we call the tree **rooted**.

Intuitively, a compact R-tree is a connected union of line segments in the plane without loops, equipped with the natural path metric.

We now show how rooted R-trees can be coded by a certain type of functions.

Definition 5.2.11: An excursion function is a continuous function $g:[0,1] \to \mathbb{R}^+$ with g(0) = g(1) = 0. For every $s, t \in [0, 1]$, define

$$m_g(s,t) := \inf_{r \in [s \wedge t, s \vee t]} g(r)$$

and

$$d_g(s,t) := g(s) + g(t) - 2m_g(s,t).$$

By the symmetric definition, we have $d_g(s,t) = d_g(t,s)$ and one can verify that the triangle inequality holds for d_q . Therefore, it is a pseudo-metric on [0, 1] and we can define the corresponding equivalence relation \sim_q by

$$s \sim_q t : \iff d_q(s,t) = 0 \iff m_q(s,t) = g(s) = g(t)$$

for $s,t\in[0,1]$. We note that, by the definition of g, we have $0\sim_g 1$. On the quotient space given by $\mathcal{T}_g := [0,1]/_{\sim_g}$, the function d_g is a metric. It can be shown that the metric space (\mathcal{T}_q, d_q) is a compact \mathbb{R} -tree. (Theorem 2.1 in [DG05]) We will view (\mathcal{T}_q, d_q) as a rooted \mathbb{R} -tree, by choosing its root to be $\rho = \pi_g(0) = \pi_g(1)$ where $\pi_g: [0,1] \to \mathcal{T}_g$ denotes the canonical projection. Furthermore, $g \mapsto \mathcal{T}_g$ is continuous from $(C([0,1], \|\cdot\|_{\infty}))$ to the space of compact \mathbb{R} -trees equipped with the Gromov-Hausdorff distance.

The encoding by an excursion function induces a (cyclic) ordering on the tree \mathcal{T}_q . Later, we want to make use of the notion of intervals that correspond to the set of vertices that are visited when going from one vertex to another in "clockwise order around the tree".

Definition 5.2.12: Let g be an excursion function and $a, b \in \mathcal{T}_g$ with $a \neq b$. Let [s, t] be the smallest interval such that $\pi_g(s) = a$ and $\pi_g(t) = b$ holds.² We then set

$$[a,b] := \pi_q([s,t]).$$

Next, we give some basic notions that are widely used in probability theory and related fields.

Definition 5.2.13: For a given probability space $(\Omega, \mathcal{F}, \mathbb{P})$, a real-valued **stochastic process** is a mapping $X : [0, \infty) \times \Omega \to \mathbb{R}$. We write $X_t = X_t(w) := X(t, w)$ and require the random variables X_t to be \mathcal{F} -measurable for each $t \geq 0$.

Note that a stochastic process is a family $(X_t)_{t\geq 0}$ of random variable; in many applications, the variable t has the meaning of time.

Definition 5.2.14: A real-valued stochastic process $(X_t)_{t\geq 0}$ is called a **Gaussian process** if for every finite choice of $t_1, \ldots, t_k \geq 0$, the random vector

$$(X_{t_1},\ldots,X_{t_k})$$

has a multivariate normal distribution with some mean vector and covariance matrix.

Definition 5.2.15: A real-valued stochastic process $(B_t)_{t\geq 0}$ is called a **Wiener process** (or **Brownian motion**) with start in $x \in \mathbb{R}$ if the following properties hold:

- 1. $B_0 = x$ almost surely,
- 2. for $n \in \mathbb{N}$ and all $0 \le t_1 \le t_2 \le \cdots \le t_n$, the increments $B_{t_j} B_{t_{j-1}}$ for $j = 2, \ldots, n$, are independent random variables,
- 3. for every $t \ge 0$, the increments $B_{t+u} B_t$, $u \ge 0$, are normally distributed with mean 0 and variance u,
- 4. the function $t \mapsto B_t$ is almost surely continuous.

A Brownian motion with start in 0 is called a **standard Brownian motion**.

Similarly, the Brownian motion is the universal scaling limit for many different random walks on the lattice.

The Brownian map seems to be the right model for a purely random surface, similar to how Brownian motion can be viewed as a purely random continuous curve.

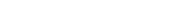
Definition 5.2.16: Let $(B_t)_{t\geq 0}$ be a standard Brownian motion. Set $\tau_+ := \inf\{t \geq 1 : B_t = 0\}$ and $\tau_- := \sup\{t \leq 1 : B_t = 0\}$. The stochastic process $(B_t)_{\tau_- \leq t \leq \tau_+}$ is called the **Brownian excursion**. The stochastic process defined by

$$\mathbf{e} := (e_t)_{0 \le t \le 1} = \left(\frac{|B_{\tau_- + t(\tau_+ - \tau_-)}|}{\sqrt{\tau_+ - \tau_-}}\right)_{0 \le t \le 1}$$

66

is called the standard Brownian excursion

²With the convention that $[s,t] := [s,1] \cup [0,t]$ if s > t.



It is important to note that $\tau_- < 1 < \tau_+$ almost surely since $B_0 = 0$ and $W_1 \neq 0$ almost surely Thus, a Brownian excursion process is basically a Brownian motion conditioned to be positive on (0,1) and to return to the value 0 at t=1.

It is a classical result (see [Ald93; GM12]) that the normalized contour function of a uniform random plane tree with n edges converges in distribution to the normalized Brownian excursion.

Analogously to Definition 5.2.11, we can also define random R-trees from random continuous functions that satisfy the properties of an excursion function. We specify such a random \mathbb{R} -tree for a special kind of random continuous function.

Definition 5.2.17: The Continuum Random Tree (CRT) is the random compact \mathbb{R} -tree $(\mathcal{T}_{\mathbf{e}}, d_{\mathbf{e}})$ coded by the normalized Brownian excursion \mathbf{e} .

Theorem 5.2.18: The Hausdorff dimension $\dim_{\mathbf{H}}(\mathcal{T}_{e})$ of the CRT (\mathcal{T}_{e}, d_{e}) is almost surely equal to 2.

In order to perform a similar strategy as in the CVS bijection, we need something like labels on the CRT. Consider first a (deterministic) \mathbb{R} -tree (\mathcal{T},d) rooted at ρ , and the real-valued centered Gaussian process $\mathcal{Z} = (\mathcal{Z}_a)_{a \in \mathcal{T}}$ whose distribution is determined by $\mathcal{Z}_{\rho} = 0$ and $E[(\mathcal{Z}_a - \mathcal{Z}_b)^2] = d(a,b)$ for $a,b \in \mathcal{T}$. In a very similar way, we can construct such a process $Z = (Z_a)_{a \in \mathcal{T}_e}$ from the CRT (\mathcal{T}_e, d_e) . Since we consider a random process Z indexed by a random set $\mathcal{T}_{\mathbf{e}}$, we need to be a bit careful. A rigorous construction of the process Z can be done via the theory of the Brownian snake (we refer to [Gal99] for an introduction).

We now present a continuous analog of the right side of the distance bound in discrete graphs (3.4):

For every $a, b \in \mathcal{T}_{\mathbf{e}}$, we set

$$D^{\circ}(a,b) := Z_a + Z_b - 2 \max \left(\min_{c \in [a,b]} Z_c, \min_{c \in [b,a]} Z_c \right).$$

The function D° does not satisfy the triangle inequality and thus, does not serve as a pseudo-metric on $\mathcal{T}_{\mathbf{e}}$. On the other hand, we can define another function³ by

$$D(a,b) := \inf\{\sum_{i=1}^k D^{\circ}(a_{i-1},a_i)\}$$

for every $a, b \in \mathcal{T}_{\mathbf{e}}$, where the infimum is taken over all finite sequences $a_0, a_1, \ldots, a_{k-1}, a_k$ of $\mathcal{T}_{\mathbf{e}}$ with $a_0 = a$ and $a_k = b$. Now, D is a pseudo-metric on $\mathcal{T}_{\mathbf{e}}$, and we can consider the corresponding equivalence relation \approx with $a \approx b$ if and only if D(a,b) = 0 for every $a, b \in \mathcal{T}_{\mathbf{e}}$.

Definition 5.2.19: The Brownian map is the quotient space $\mathbf{m}_{\infty} := \mathcal{T}_{\mathbf{e}}/_{\approx}$ equipped with the distance induced by D.

³In fact, the function D is the largest symmetric function that has D° as upper bound and satisfies the triangle inequality.

If we write $\Pi: \mathcal{T}_{\mathbf{e}} \to \mathbf{m}_{\infty}$ for the canonical projection, and keep the notation D for the induced distance on \mathbf{m}_{∞} , one can prove the following using Theorem 3.4 in [Le 07].

Proposition 5.2.20: For every $a, b \in \mathcal{T}_e$, we have almost surely

$$D(a,b) = 0 \iff D^{\circ}(a,b) = 0 \iff Z_a = Z_b = \max\left(\min_{c \in [a,b]} Z_c, \min_{c \in [b,a]} Z_c\right).$$

Proposition 5.2.20 implies that two vertices a, b of the CRT are equivalent under \approx and are thus identified in the Brownian map if they have equal labels $Z_a = Z_b$ and if there exists a (clockwise or counterclockwise) "tour around the tree" where only vertices with label greater than or equal to $Z_a = Z_b$ are encountered. In fact, only certain leaves of the CRT are identified under \approx , and the set of these leaves has Hausdorff dimension 1, whereas the CRT itself can be shown to have Hausdorff dimension 2. Moreover, every equivalence class of \approx contains at most 3 vertices, and there are only countably many equivalence classes consisting of exactly 3 points.

The Brownian map exhibits various properties that distinguish it from a smooth surface.

Theorem 5.2.21: The Hausdorff dimension of the Brownian map is almost surely equal to 4. The Brownian map is almost surely homeomorphic to the sphere \mathbb{S}^2 .

The proof of the first statement can be found in Theorem 6.1 of [Le 07], the proof of the second statement can be found in Chapter 3 of [GP06].

References

- [Ald93] David Aldous. "The Continuum Random Tree III". In: The Annals of Probability 21.1 (1993), pp. 248-289. DOI: 10.1214/aop/1176989404. URL: https: //doi.org/10.1214/aop/1176989404.
- [AP15] Marie Albenque and Dominique Poulalhon. Generic method for bijections between blossoming trees and planar maps. 2015. arXiv: 1305.1312 [math.CO]. URL: https://arxiv.org/abs/1305.1312.
- [BBI01] Dmitri Burago, Yuri Burago, and Sergei Ivanov. "A Course in Metric Geometry". In: Graduate Studies in Math. 33 (Jan. 2001).
- [BC11] Olivier Bernardi and Guillaume Chapuy. A bijection for covered maps, or a shortcut between Harer-Zagier's and Jackson's formulas. 2011. arXiv: 1001. 1592 [math.CO]. URL: https://arxiv.org/abs/1001.1592.
- [BC91] Edward A Bender and E.Rodney Canfield. "The number of rooted maps on an orientable surface". In: Journal of Combinatorial Theory, Series B 53.2 (1991), pp. 293-299. ISSN: 0095-8956. DOI: https://doi.org/10.1016/0095-8956(91) 90079-Y. URL: https://www.sciencedirect.com/science/article/pii/ 009589569190079Y.
- Olivier Bernardi. Bijective counting of tree-rooted maps and shuffles of paren-[Ber06] thesis systems. 2006. arXiv: math/0601684 [math.CO]. URL: https://arxiv. org/abs/math/0601684.
- [BF11] Olivier Bernardi and Eric Fusy. A bijection for triangulations, quadrangulations, pentagulations, etc. 2011. arXiv: 1007.1292 [math.CO]. URL: https://arxiv. org/abs/1007.1292.
- [BF12] Olivier Bernardi and Eric Fusy. Unified bijections for maps with prescribed degrees and girth. 2012. arXiv: 1102.3619 [math.CO]. URL: https://arxiv.org/ abs/1102.3619.
- [BFG04] J. Bouttier, P. Di Francesco, and E. Guitter. Planar maps as labeled mobiles. 2004. arXiv: math/0405099 [math.CO]. URL: https://arxiv.org/abs/math/ 0405099.
- [CD17] Guillaume Chapuy and Maciej Dolega. "A bijection for rooted maps on general surfaces". In: Journal of Combinatorial Theory, Series A 145 (Jan. 2017), pp. 252-307. ISSN: 0097-3165. DOI: 10.1016/j.jcta.2016.08.001. URL: http://dx.doi.org/10.1016/j.jcta.2016.08.001.
- [Cha08] Guillaume Chapuy. Asymptotic enumeration of constellations and related families of maps on orientable surfaces. 2008. arXiv: 0805.0352 [math.CO]. URL: https://arxiv.org/abs/0805.0352.

- [CMS08] Guillaume Chapuy, Michel Marcus, and Gilles Schaeffer. A bijection for rooted maps on orientable surfaces. 2008. arXiv: 0712.3649 [math.CO]. URL: https: //arxiv.org/abs/0712.3649.
- [CS02]Philippe Chassaing and Gilles Schaeffer. Random Planar Lattices and Integrated SuperBrownian Excursion. 2002. arXiv: math/0205226 [math.CO]. URL: https: //arxiv.org/abs/math/0205226.
- [CV81] Robert Cori and Bernard Vauquelin. "Planar Maps are Well Labeled Trees". In: Canadian Journal of Mathematics 33.5 (1981), pp. 1023–1041. DOI: 10.4153/ CJM-1981-078-2.
- [DG05]Thomas Duquesne and Jean-Francois Le Gall. Probabilistic and fractal aspects of Levy trees. 2005. arXiv: math/0501079 [math.PR]. URL: https://arxiv. org/abs/math/0501079.
- Reinhard Diestel. Graph Theory. 5th. Springer Publishing Company, Incorpo-[Die17] rated, 2017. ISBN: 3662536218.
- [DL22]Maciej Dolega and Mathias Lepoutre. "Blossoming bijection for bipartite pointed maps and parametric rationality of general maps of any surface". In: Advances in Applied Mathematics 141 (2022), p. 102408. ISSN: 0196-8858. DOI: https:// doi.org/10.1016/j.aam.2022.102408. URL: https://www.sciencedirect. com/science/article/pii/S0196885822000926.
- [EPW04] Steven N. Evans, Jim Pitman, and Anita Winter. Rayleigh processes, real trees, and root growth with re-grafting. 2004. arXiv: math/0402293 [math.PR]. URL: https://arxiv.org/abs/math/0402293.
- [Fel04] Stefan Felsner. "Lattice Structures from Planar Graphs". In: Electron. J. Comb. 11 (2004). URL: https://api.semanticscholar.org/CorpusID:15367239.
- [FPS08] Eric Fusy, Dominique Poulalhon, and Gilles Schaeffer. Dissections, orientations, and trees, with applications to optimal mesh encoding and to random sampling. 2008. arXiv: 0810.2608 [math.CO]. URL: https://arxiv.org/abs/0810.2608.
- [FS09] Philippe Flajolet and Robert Sedgewick. Analytic Combinatorics. 1st ed. USA: Cambridge University Press, 2009. ISBN: 0521898064.
- [Gal14] Jean-François Le Gall. Random geometry on the sphere. 2014. arXiv: 1403.7943 [math.PR]. URL: https://arxiv.org/abs/1403.7943.
- [Gal99] Jean-Francois Le Gall. Spatial Branching Processes, Random Snakes and Partial Differential Equations. eng. 1st ed. 1999. Lectures in Mathematics. ETH Zürich. Basel: Birkhäuser Basel, 1999. ISBN: 3-0348-8683-7.
- [GM12]Jean-François Le Gall and Grégory Miermont. Scaling limits of random trees and planar maps. 2012. arXiv: 1101.4856 [math.PR]. URL: https://arxiv. org/abs/1101.4856.
- [GP06] J. F. Le Gall and F. Paulin. Scaling limits of bipartite planar maps are homeomorphic to the 2-sphere. 2006. arXiv: math/0612315 [math.PR]. URL: https: //arxiv.org/abs/math/0612315.

- [Jan11] Svante Janson. Simply generated trees, conditioned Galton-Watson trees, random allocations and condensation. 2011. arXiv: 1112.0510 [math.PR]. URL: https://arxiv.org/abs/1112.0510.
- Jean-François Le Gall. "The topological structure of scaling limits of large pla-[Le 07] nar maps". In: Inventiones mathematicae 169.3 (June 2007), pp. 621–670. ISSN: 1432-1297. DOI: 10.1007/s00222-007-0059-9. URL: http://dx.doi.org/10. 1007/s00222-007-0059-9.
- [Le 13] Jean-François Le Gall. "Uniqueness and universality of the Brownian map". In: The Annals of Probability 41.4 (July 2013). ISSN: 0091-1798. DOI: 10.1214/12aop792. URL: http://dx.doi.org/10.1214/12-AOP792.
- [Lep19] Mathias Lepoutre. "Blossoming bijection for higher-genus maps". In: Journal of Combinatorial Theory, Series A 165 (2019), pp. 187–224. ISSN: 0097-3165. DOI: https://doi.org/10.1016/j.jcta.2019.01.005. URL: https://www. sciencedirect.com/science/article/pii/S0097316519300068.
- [Mie13] Grégory Miermont. "The Brownian map is the scaling limit of uniform random plane quadrangulations". In: Acta Mathematica 210.2 (2013), pp. 319–401. DOI: 10.1007/s11511-013-0096-8. URL: https://doi.org/10.1007/s11511-013-0096-8.
- [MS01] Michel Marcus and Gilles Schaeffer. "Une bijection simple pour les cartes orientables". In: 2001. URL: https://api.semanticscholar.org/CorpusID: 118593294.
- [MT01] Bojan Mohar and Carsten Thomassen. Graphs on Surfaces. Johns Hopkins series in the mathematical sciences. Johns Hopkins University Press, 2001, pp. I-XI, 1-291. ISBN: 978-0-8018-6689-0.
- [PS06] Dominique Poulalhon and Gilles Schaeffer. "Optimal Coding and Sampling of Triangulations". In: Algorithmica 46.3–4 (Nov. 2006), pp. 505–527. ISSN: 0178-4617.
- [Sch97] Gilles Schaeffer. "Bijective census and random generation of Eulerian planar maps with prescribed vertex degrees". In: 1997. URL: https://api.semanticscholar. org/CorpusID:7180358.
- [Sch98] Gilles Schaeffer. "Conjugaison d'arbres et cartes combinatoires aléatoires". In: 1998. URL: https://api.semanticscholar.org/CorpusID:170748288.
- [Tho92] Carsten Thomassen. "The Jordan-Scho" nflies theorem and the classification of surfaces". In: Am. Math. Monthly 99.2 (Feb. 1992), pp. 116–130. ISSN: 0002-9890. DOI: 10.2307/2324180. URL: https://doi.org/10.2307/2324180.
- [Tut63] William T. Tutte. "A Census of Planar Maps". In: Canadian Journal of Mathematics 15 (1963), pp. 249-271. URL: https://api.semanticscholar.org/ CorpusID: 122188928.
- [Wal72] David W. Walkup. "The number of plane trees". In: Mathematika 19.2 (1972), pp. 200-204. DOI: 10.1112/S0025579300005659.